On the Synthesis of modular phased arrays exploiting diamond tiles

P. Rocca, N. Anselmi, A. Polo, and A. Massa

Contents

1 Numerical Results

1.1 ETM - Hexagon (2,2,2) - Min SLL

Array Geometry

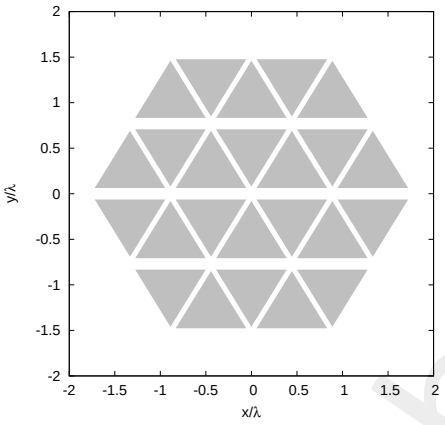

Figure 1: $N_{tot} = 24,\ L_d = 4\lambda,\ d_x = 0.44\lambda,\ d_{y1} = 0.51\lambda,\ d_{y2} = \lambda,\ N_c^{tot} = 32,\ N_p^{tot} = 25,\ N_p^{(bound)} = 13,\ a = 2,\ b = 2,\ c = 2$ − Array Geometry

Reference Array, Convex Programming Excitations

Test case parameters

The parameters are:

- Number of array elements - $N_{tot} = 24$
- Element spacing along x - $d_x = 0.44\lambda$
- Element spacing along y_1 - $d_{y1} = 0.51\lambda$
- Element spacing along y_2 - $d_{y2} = \lambda$
- Pointing Direction - $\theta_0 = 0^\circ$
- Pointing Direction - $\phi_0 = 0^\circ$
- Pointing Direction - $u_0 = 0$
- Pointing Direction - $v_0 = 0$
- A side length - $a = 2$
- B side length - $b = 2$
- C side length - $c = 2$

Array Tiling

Goal

Applying ETM algorithm with lozenge tiles encoded as integer strings.

Software Parameters

The parameters are:

- Number of array elements - $N_{tot} = 24$
- Element spacing along x - $d_x = 0.44\lambda$
- Element spacing along y_1 - $d_{y1} = 0.51\lambda$
- Element spacing along y_2 - $d_{y2} = \lambda$
- Side's domain - $L_d = 4\lambda$
- Points number - $N_p^{tot} = 25$
- Points along x - $M_p = 5$
- Points along y - $N_p = 5$
- Total cells number - $N_c^{tot} = 32$
- Cells along x - $M_c = 8$
- Cells along y - $N_c = 4$
- Boundary points - $N_p^{(bound)} = 13$
- Samples along u - $N_u = 250$
- Samples along v - $N_v = 250$
- SLL weight - $w_{SLL} = 1.0$
- Directivity weight - $w_D = 0$
- HPBW weight azimuth - $w_{HPBW}^{azm} = 0.0$
- HPBW weight elevation - $w_{HPBW}^{elv} = 0.0$
- Mask weight - $w_{mask} = 0.0$
- Cell elements - $N_{el} = 1$
- Pointing Direction - $\theta_0 = 0°$
- Pointing Direction - $\phi_0 = 0°$

- Pointing Direction - $u_0 = 0$
- Pointing Direction - $v_0 = 0$
- A side length - $a = 2$
- B side length - $b = 2$
- C side length - $c = 2$
- A side length in λ - $L_a = 0.866\lambda$
- B side length in λ- $L_b = 0.866\lambda$
- C side length in λ- $L_c = 0.866\lambda$

Results

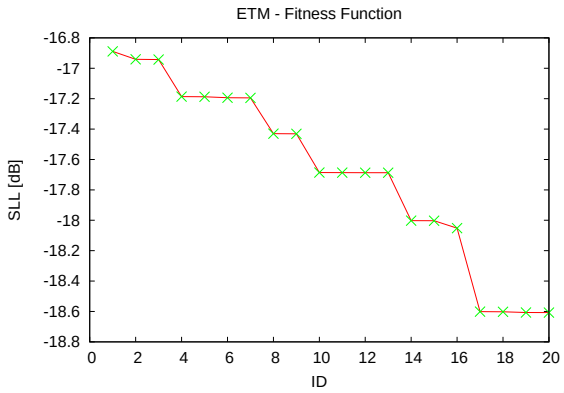

Figure 2: *CP reference excitations*, $SLL_{ref} = -19.30\ [dB]$, $N_{tot} = 24$, $L_d = 4\lambda$, $d_x = 0.44\lambda$, $d_{y1} = 0.51\lambda$, $d_{y2} = \lambda$, $a = 2$, $b = 2$, $c = 2$, $(\theta_0, \phi_0) = (0, 0)\ [deg]$ – Fitness Function

Fig. 2 rappresents the set of solutions. The maximum number of possible tiling configuration is 20. From this set, I analyze the best and the worst.

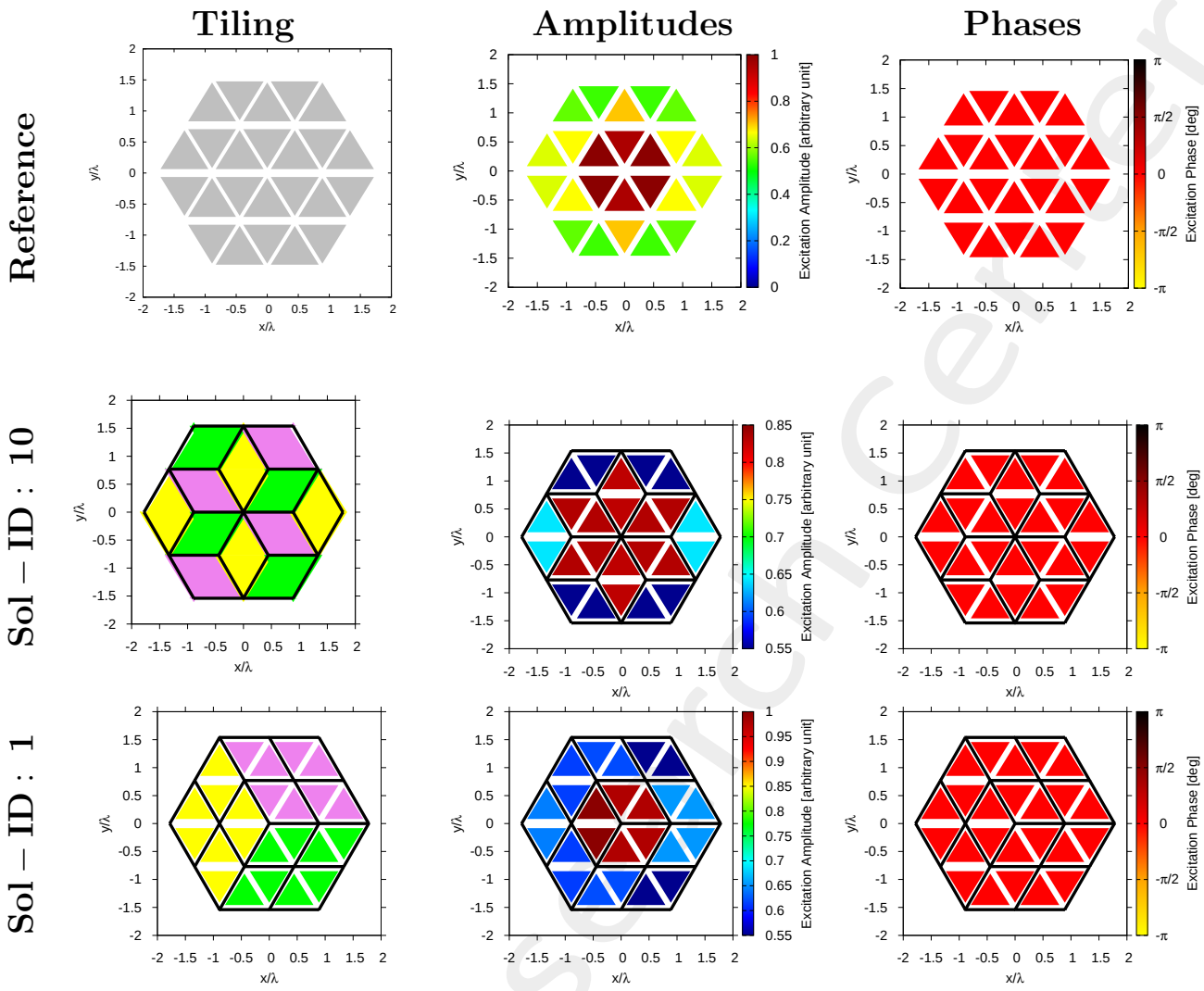

Figure 3: *CP reference excitations*, $SLL = -19.30\ [dB]$, $N_{tot} = 24$, $L_d = 4\lambda$, $d_x = 0.44\lambda$, $d_{y1} = 0.51\lambda$, $d_{y2} = \lambda$, $a = 2$, $b = 2$, $c = 2$, $(\theta_0, \phi_0) = (0, 0)\ [deg]$ – Solution ID.: Reference, 10, 1

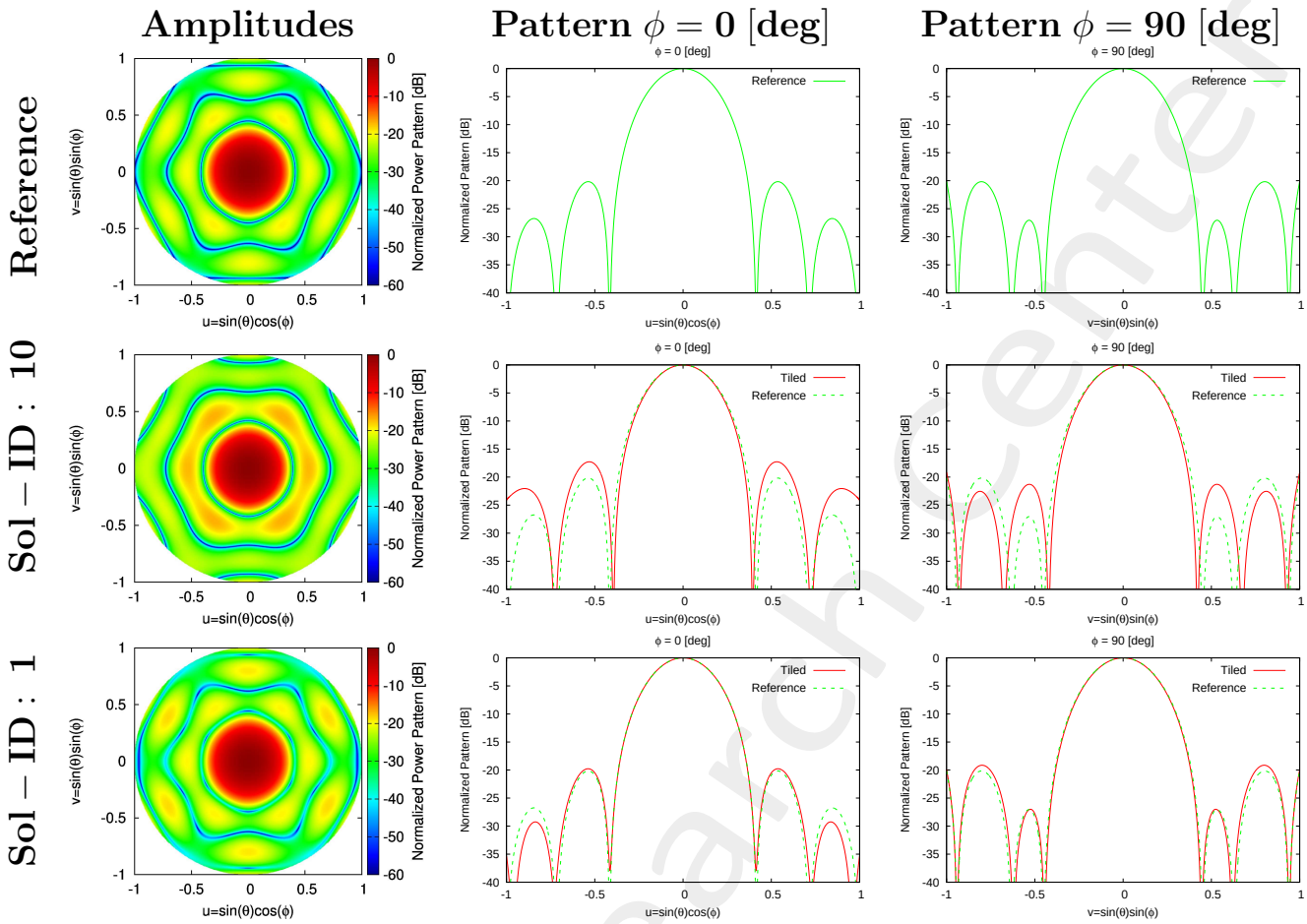

Figure 4: *CP reference excitations*, $SLL = -19.30$ $[dB]$, $N_{tot} = 24$, $L_d = 4\lambda$, $d_x = 0.44\lambda$, $d_{y1} = 0.51\lambda$, $d_{y2} = \lambda$, $a = 2$, $b = 2$, $c = 2$, $(\theta_0, \phi_0) = (0, 0)$ $[deg]$ – Solution ID.: Reference, 10, 1

Solutions Summary

(a, b, c)	**T** (# tilings)	$\triangle\tau$ $[sec]$ (single simulation period)	τ $[sec]$ total simulation period
2, 2, 2	20	0.026	0.526

Table 3: Simulation Time

SOLUTION ID	**SLL** [dB]	**HPBW** (azimuth) [deg]	**HPBW** (elevation) [deg]	**D** [dB]
Reference	−19.300	19.654	20.377	19.553
10	−16.889	19.237	19.929	19.464
1	−18.607	19.619	20.150	19.567

Table 4: SLL, $HPBW_{az}$, $HPBW_{el}$, D *of Radiation Pattern*

1.2 ETM - Hexagon (2,9,4) - Mask Matching - Steering $(\theta, \phi) = (10, 0)$ $[deg]$

Array Geometry

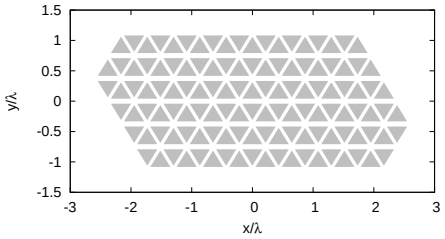

Figure 5: $N_{tot} = 124,\ L_d = 18\lambda,\ d_x = 0.22\lambda,\ d_{y1} = 0.25\lambda,\ d_{y2} = 0.5\lambda,\ N_c^{tot} = 144,\ N_p^{tot} = 91,\ N_p^{(bound)} = 31,\ a = 2,\ b = 9,\ c = 4$ − Array Geometry

Reference Array, Convex Programming Excitations

Test case parameters

The parameters are:

- Number of array elements - $N_{tot} = 124$
- Element spacing along x - $d_x = 0.22\lambda$
- Element spacing along y_1 - $d_{y1} = 0.25\lambda$
- Element spacing along y_2 - $d_{y2} = 0.5\lambda$
- Pointing Direction - $\theta_0 = 10°$
- Pointing Direction - $\phi_0 = 0°$
- Pointing Direction - $u_0 = 0.1736$
- Pointing Direction - $v_0 = 0$
- A side length - $a = 2$
- B side length - $b = 9$
- C side length - $c = 4$

Mask Constraints

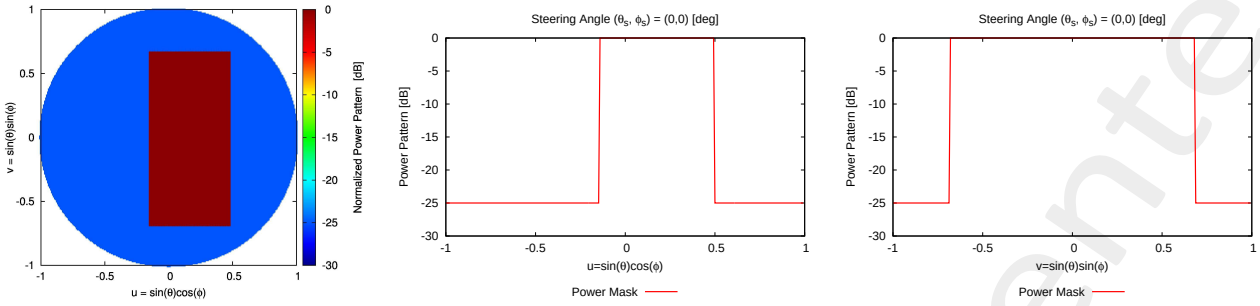

(a) *(b)* *(c)*

Figure 6: Mask Power Pattern steering direction $(\theta, \phi) = (10, 0)$ $[deg]$: (a) 2D, (b) Normalized cut along azimuth direction, (c) Normalized cut along elevation direction.

Array Tiling

Goal

Applying ETM algorithm with lozenge tiles encoded as integer strings.

Software Parameters

The parameters are:

- Number of array elements - $N_{tot} = 124$
- Element spacing along x - $d_x = 0.22\lambda$
- Element spacing along y_1 - $d_{y1} = 0.25\lambda$
- Element spacing along y_2 - $d_{y2} = 0.5\lambda$
- Side's domain - $L_d = 18\lambda$
- Points number - $N_p^{tot} = 91$
- Points along x - $M_p = 13$
- Points along y - $N_p = 7$
- Total cells number - $N_c^{tot} = 144$
- Cells along x - $M_c = 24$
- Cells along y - $N_c = 6$
- Boundary points - $N_p^{(bound)} = 31$
- Samples along u - $N_u = 256$

- Samples along v - $N_v = 256$
- SLL weight - $w_{SLL} = 0.0$
- Directivity weight - $w_D = 0$
- HPBW weight azimuth - $w_{HPBW}^{azm} = 0.0$
- HPBW weight elevation - $w_{HPBW}^{elv} = 0.0$
- Mask weight - $w_{mask} = 1.0$
- Cell elements - $N_{el} = 1$
- Pointing Direction - $\theta_0 = 10°$
- Pointing Direction - $\phi_0 = 0°$
- Pointing Direction - $u_0 = 0.1736$
- Pointing Direction - $v_0 = 0$
- A side length - $a = 2$
- B side length - $b = 9$
- C side length - $c = 4$
- A side length in λ - $L_a = 0.866\lambda$
- B side length in λ- $L_b = 3.897\lambda$
- C side length in λ- $L_c = 1.732\lambda$

Results

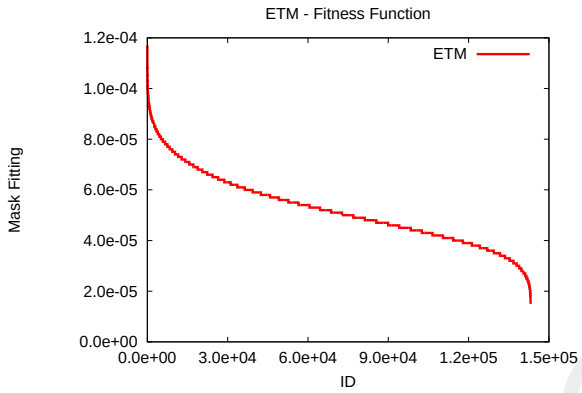

Figure 7: *Mask Matching*, $N_{tot} = 124$, $L_d = 18\lambda$, $d_x = 0.22\lambda$, $d_{y1} = 0.25\lambda$, $d_{y2} = 0.5\lambda$, $a = 2$, $b = 9$, $c = 4$, $(\theta_0, \phi_0) = (0, 0)$ $[deg]$ – Fitness Function

Fig. 7 rappresents the set of solutions. The maximum number of possible tiling configuration is 143143. From this set, I analyze the best and the worst.

Broadside Analysis

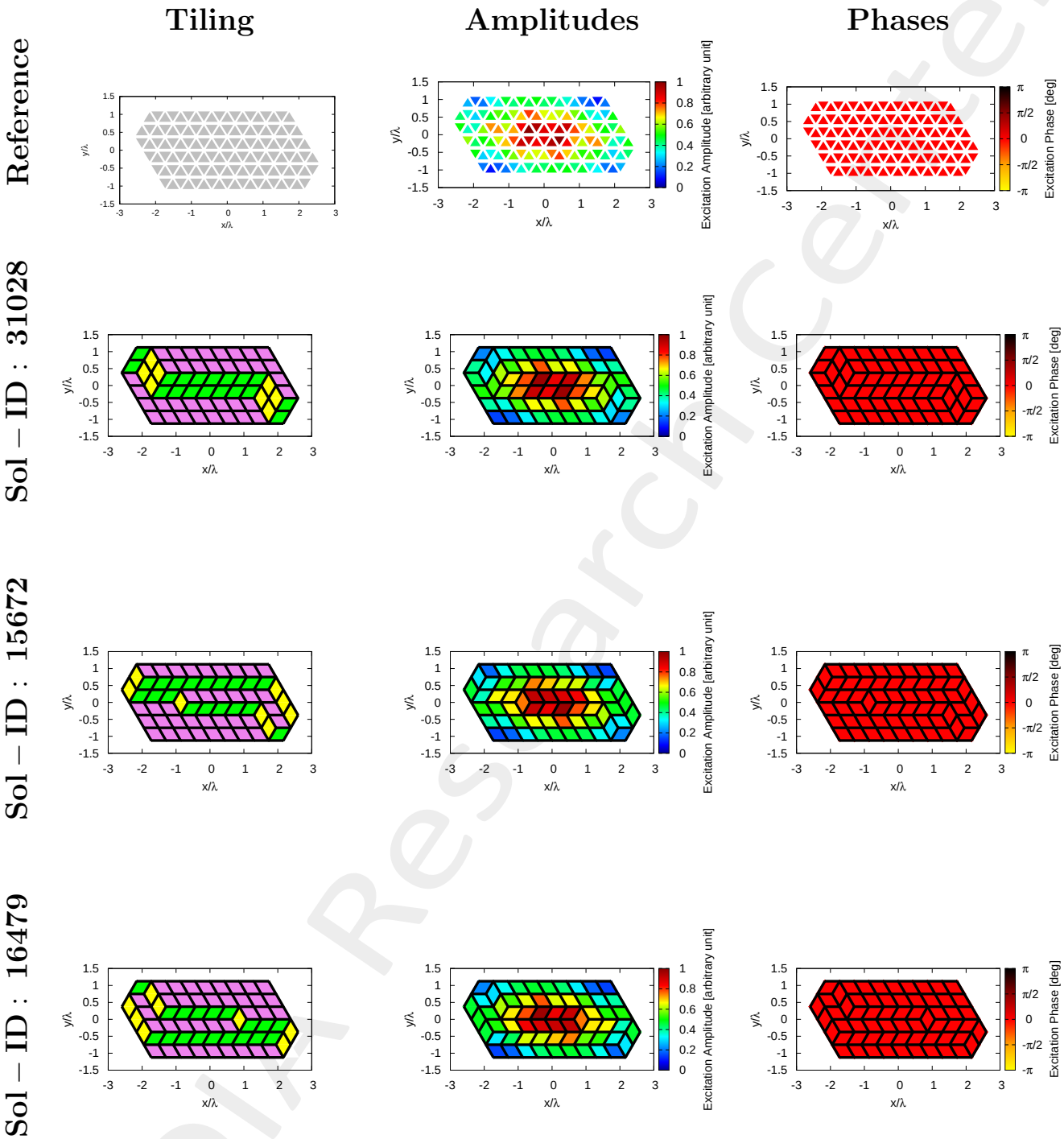

Figure 8: *Mask Matching*, $SLL = -24.97\ [dB]$, $N_{tot} = 124$, $L_d = 18\lambda$, $d_x = 0.22\lambda$, $d_{y1} = 0.25\lambda$, $d_{y2} = 0.5\lambda$, $a = 2$, $b = 9$, $c = 4$, $(\theta_0, \phi_0) = (0, 0)\ [deg]$ – Solution ID.: Reference, 31028, 15672, 16479

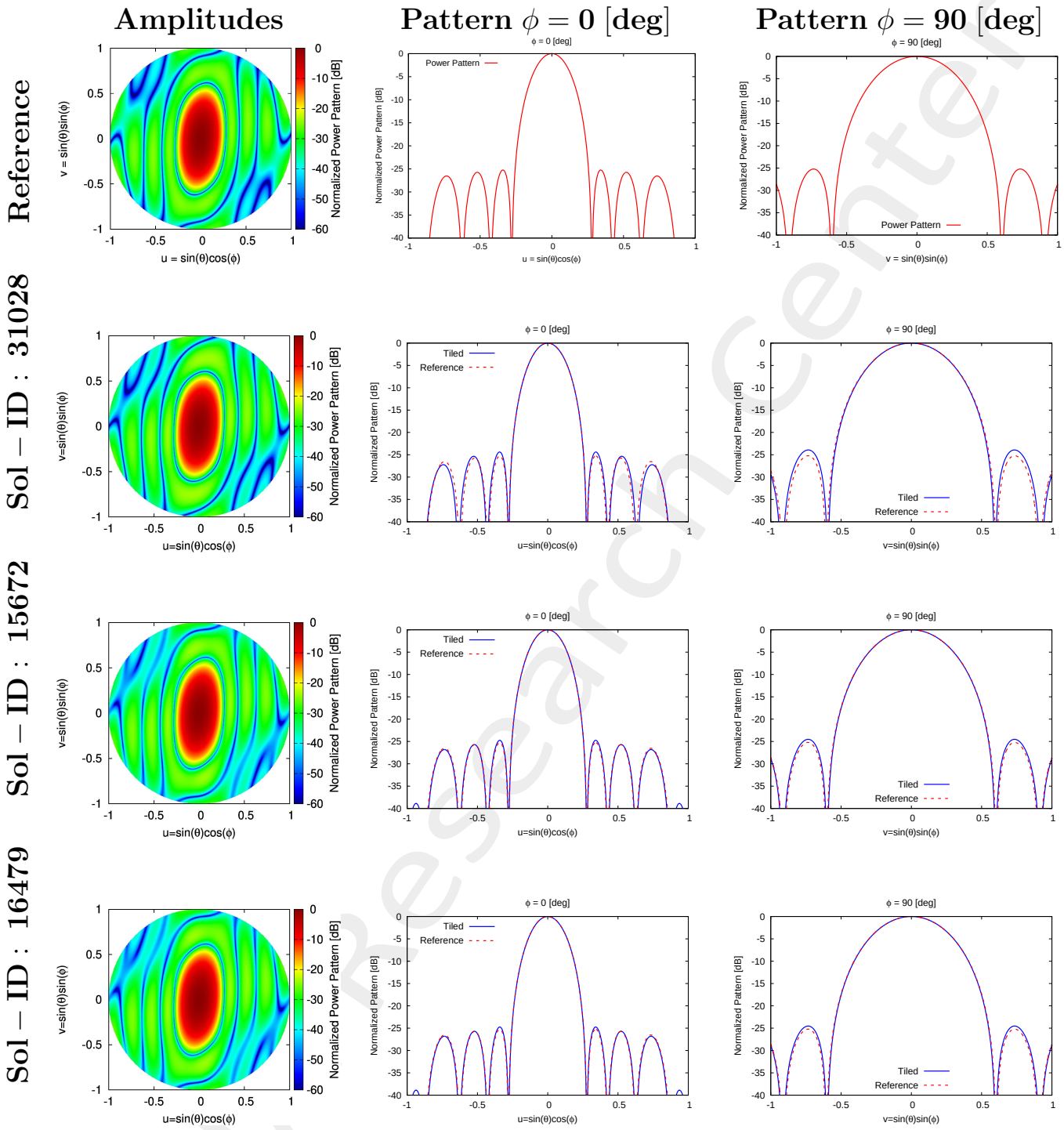

Figure 9: *Mask Matching*, $SLL = -24.97$ $[dB]$, $N_{tot} = 124$, $L_d = 18\lambda$, $d_x = 0.22\lambda$, $d_{y1} = 0.25\lambda$, $d_{y2} = 0.5\lambda$, $a = 2$, $b = 9$, $c = 4$, $(\theta_0, \phi_0) = (0, 0)$ $[deg]$ – Solution ID.: Reference, 31028, 15672, 16479

Steering Analysis

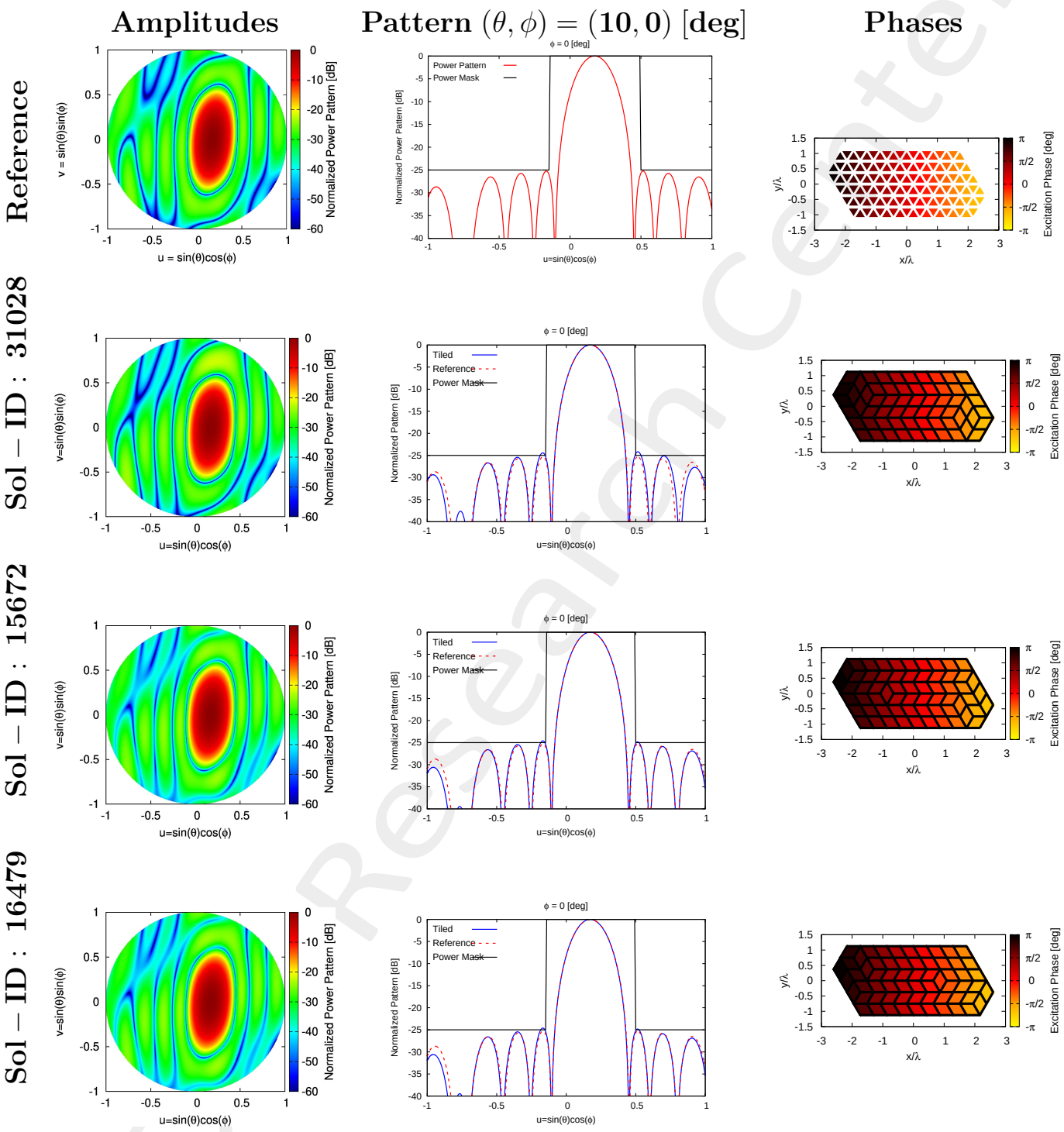

Figure 10: *Mask Matching*, $SLL = -24.97$ $[dB]$, $N_{tot} = 124$, $L_d = 18\lambda$, $d_x = 0.22\lambda$, $d_{y1} = 0.25\lambda$, $d_{y2} = 0.5\lambda$, $a = 2$, $b = 9$, $c = 4$, $(\theta_0, \phi_0) = (10, 0)$ $[deg]$ – Solution ID.: Reference, 31028, 15672, 16479

Solutions Summary

(a, b, c)	**T** (# tilings)	$\triangle\tau$ $[sec]$ (single simulation period)	τ $[sec]$ total simulation period
2, 9, 4	143143	0.12365	1770007

Table 9: Simulation Time

SOLUTION ID	**SLL** [dB]	**HPBW** (azimuth) [deg]	**HPBW** (elevation) [deg]	**D** [dB]	**Mask Fitting**
Reference	−24.974	12.580	27.536	20.335	0
31028	−23.838	12.610	27.399	20.342	1.17×10^{-4}
15672	−24.109	12.569	27.472	20.348	1.499×10^{-5}
16479	−24.109	12.569	27.472	20.348	1.499×10^{-5}

Table 10: SLL, $HPBW_{az}$, $HPBW_{el}$, D, *Mask Fitting of Radiation Pattern* along $(\theta_0, \phi_0) = (0, 0)$ [deg]

1.3 ETM - Hexagon (4,4,4) - Mask Matching - Broadside - $d_{y2} = 0.77\lambda$

Array Geometry

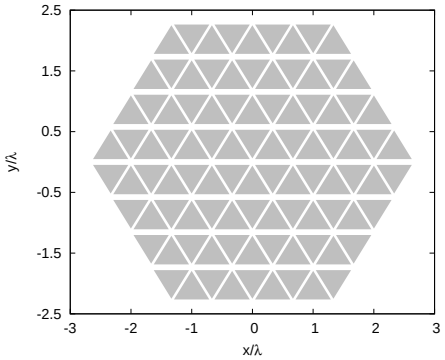

Figure 11: $N_{tot} = 96,\ L_d = 8\lambda,\ d_x = 0.334\lambda,\ d_{y1} = 0.385\lambda,\ d_{y2} = 0.77\lambda,\ N_c^{tot} = 128,\ N_p^{tot} = 81,\ N_p^{(bound)} = 25,\ a = 4,\ b = 4,\ c = 4$ − Array Geometry

Reference Array, Convex Programming Excitations

Test case parameters

The parameters are:

- Number of array elements - $N_{tot} = 96$
- Element spacing along x - $d_x = 0.334\lambda$
- Element spacing along y_1 - $d_{y1} = 0.385\lambda$
- Element spacing along y_2 - $d_{y2} = 0.77\lambda$
- Pointing Direction - $\theta_0 = 0°$
- Pointing Direction - $\phi_0 = 0°$
- Pointing Direction - $u_0 = 0$
- Pointing Direction - $v_0 = 0$
- A side length - $a = 4$
- B side length - $b = 4$
- C side length - $c = 4$

Mask Constraints

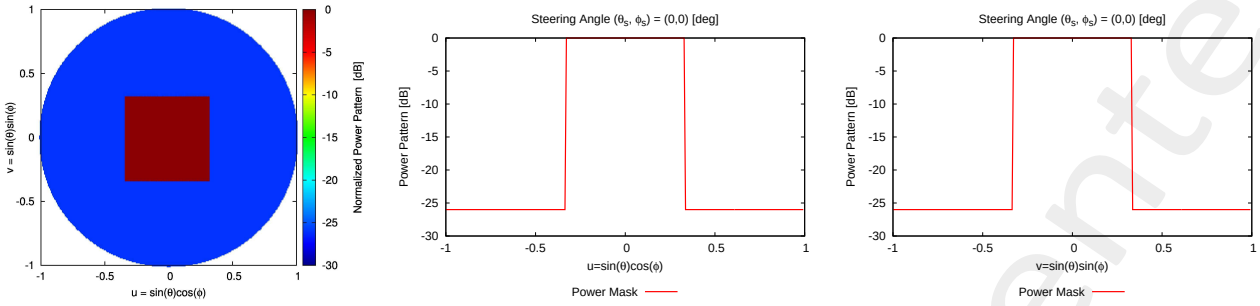

(a) *(b)* *(c)*

Figure 12: Mask Power Pattern in broadside direction $(\theta, \phi) = (0, 0)$ $[deg]$: (a) 2D, (b) Normalized cut along azimuth direction, (c) Normalized cut along elevation direction.

Array Tiling

Goal

Applying ETM algorithm with lozenge tiles encoded as integer strings.

Software Parameters

The parameters are:

- Number of array elements - $N_{tot} = 96$
- Element spacing along x - $d_x = 0.334\lambda$
- Element spacing along y_1 - $d_{y1} = 0.385\lambda$
- Element spacing along y_2 - $d_{y2} = 0.77\lambda$
- Side's domain - $L_d = 8\lambda$
- Points number - $N_p^{tot} = 81$
- Points along x - $M_p = 9$
- Points along y - $N_p = 9$
- Total cells number - $N_c^{tot} = 128$
- Cells along x - $M_c = 16$
- Cells along y - $N_c = 8$
- Boundary points - $N_p^{(bound)} = 25$
- Samples along u - $N_u = 256$

- Samples along v - $N_v = 256$
- SLL weight - $w_{SLL} = 0.0$
- Directivity weight - $w_D = 0$
- HPBW weight azimuth - $w_{HPBW}^{azm} = 0.0$
- HPBW weight elevation - $w_{HPBW}^{elv} = 0.0$
- Mask weight - $w_{mask} = 1.0$
- Cell elements - $N_{el} = 1$
- Pointing Direction - $\theta_0 = 0°$
- Pointing Direction - $\phi_0 = 0°$
- Pointing Direction - $u_0 = 0$
- Pointing Direction - $v_0 = 0$
- A side length - $a = 4$
- B side length - $b = 4$
- C side length - $c = 4$
- A side length in λ - $L_a = 2.668\lambda$
- B side length in λ- $L_b = 2.668\lambda$
- C side length in λ- $L_c = 2.668\lambda$

Results

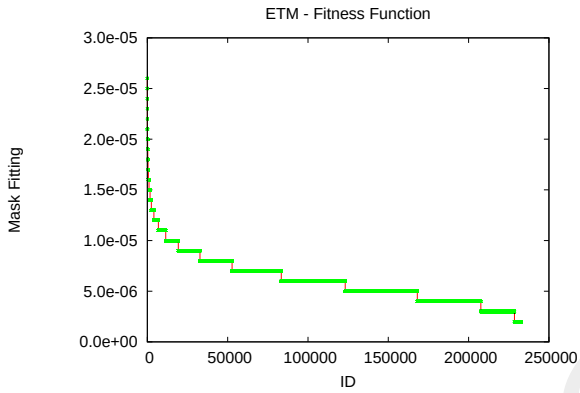

Figure 13: *Mask Matching*, $N_{tot} = 96$, $L_d = 8\lambda$, $d_x = 0.334\lambda$, $d_{y1} = 0.385\lambda$, $d_{y2} = 0.77\lambda$, $a = 4$, $b = 4$, $c = 4$, $(\theta_0, \phi_0) = (0, 0)$ $[deg]$ – Fitness Function

Fig. 13 rappresents the set of solutions. The maximum number of possible tiling configuration is 232848. From this set, I analyze the best and the worst.

Broadside Analysis

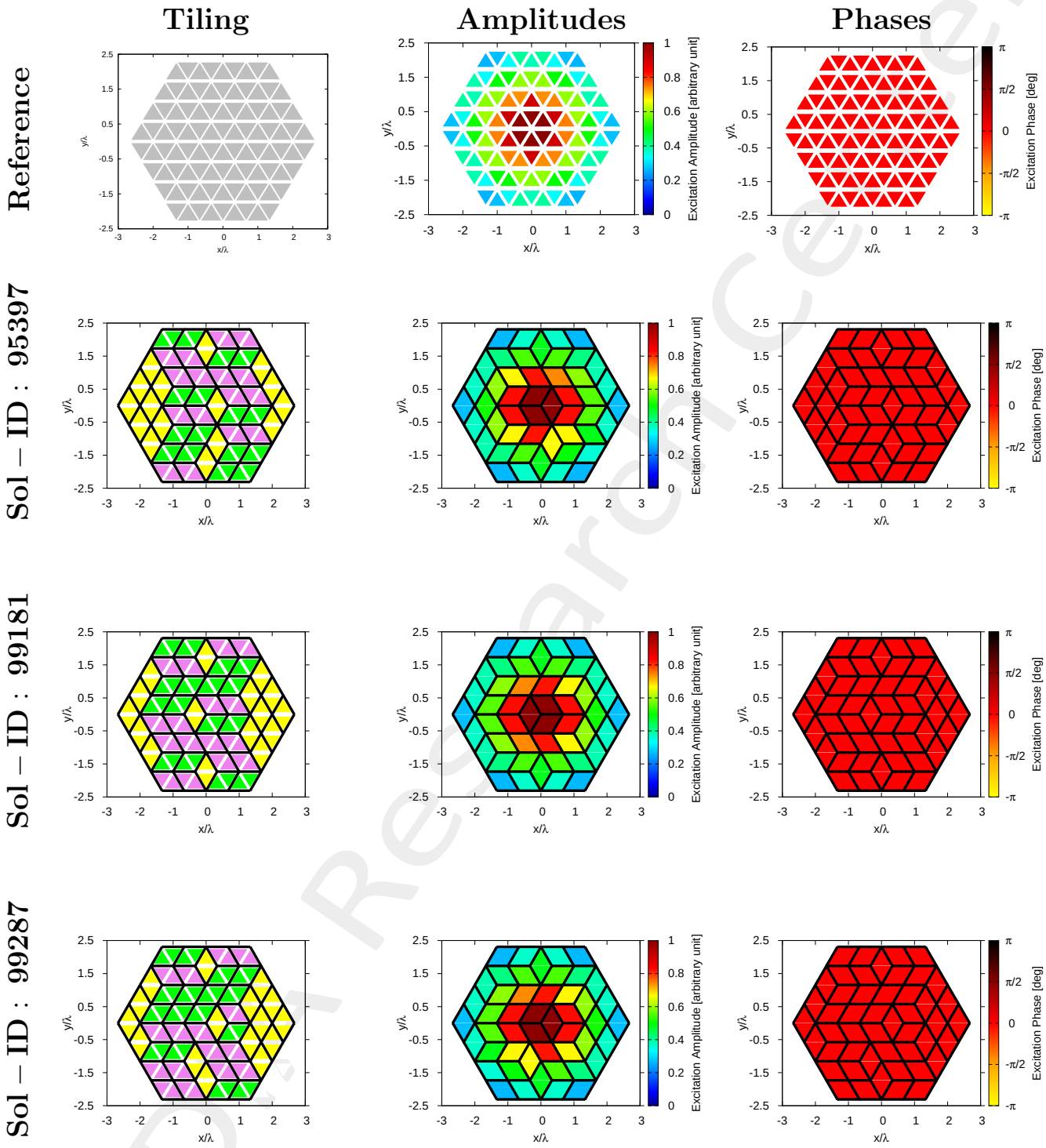

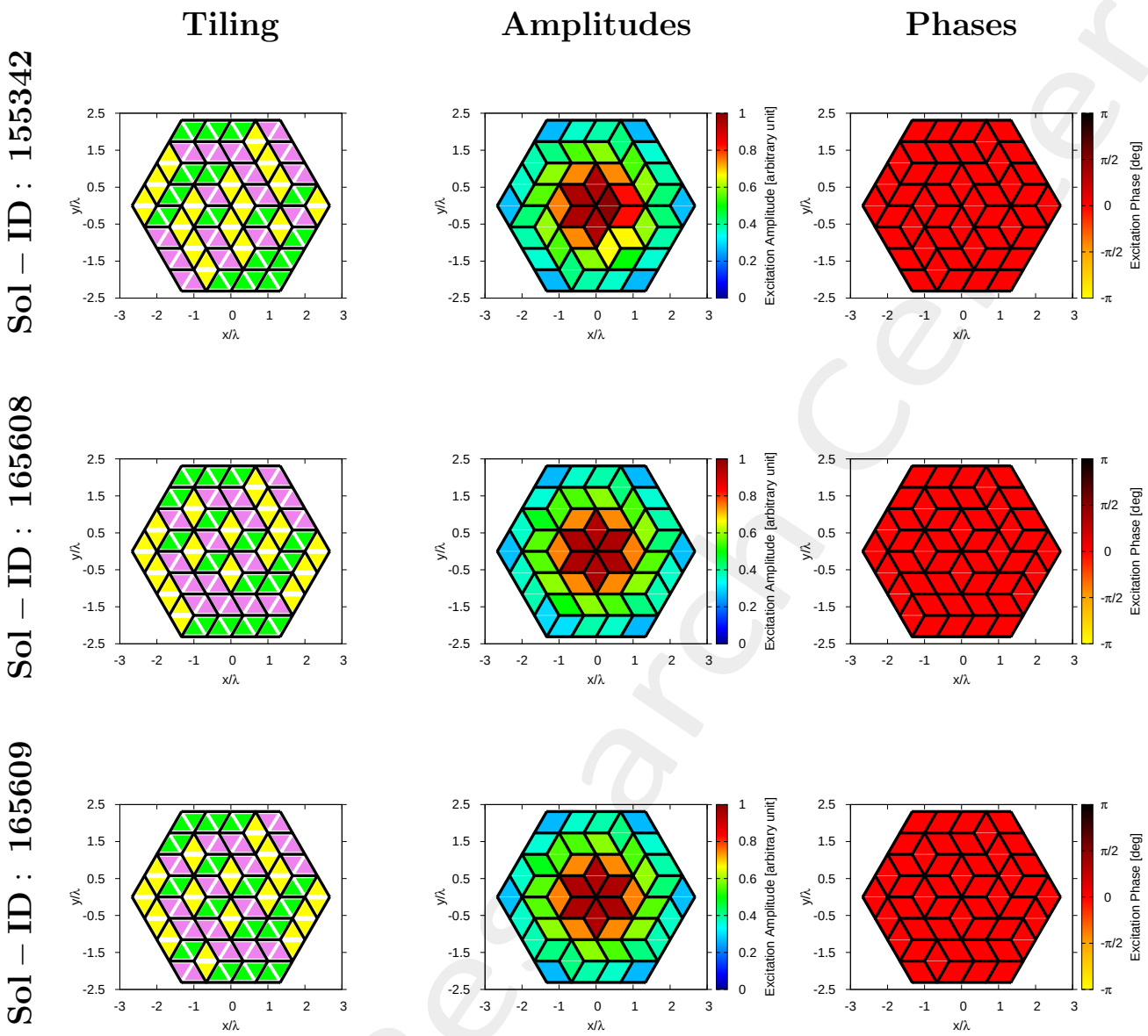

Figure 14: *Mask Matching*, $SLL = -25.99\ [dB]$, $N_{tot} = 96$, $L_d = 8\lambda$, $d_x = 0.334\lambda$, $d_{y1} = 0.385\lambda$, $d_{y2} = 0.77\lambda$, $a = 4$, $b = 4$, $c = 4$, $(\theta_0, \phi_0) = (0, 0)\ [deg]$ – Solution ID.: Reference, 95397, 99181, 99287, 155342, 165608, 165609

	Amplitudes	Pattern $\phi = 0$ [deg]	Pattern $\phi = 90$ [deg]
Reference	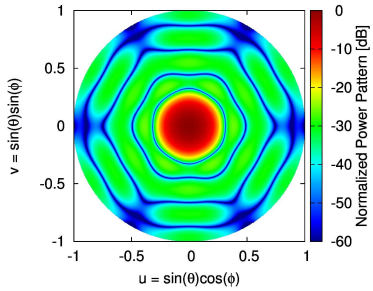	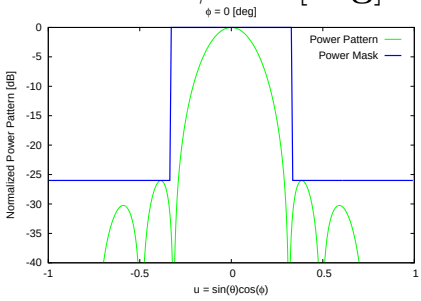	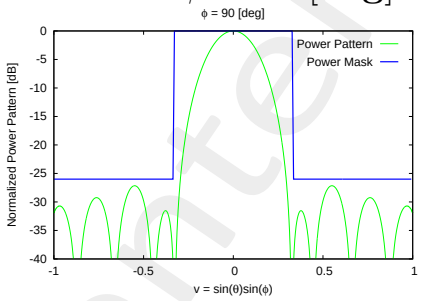
Sol – ID : 95397	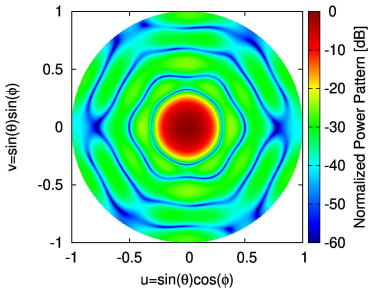	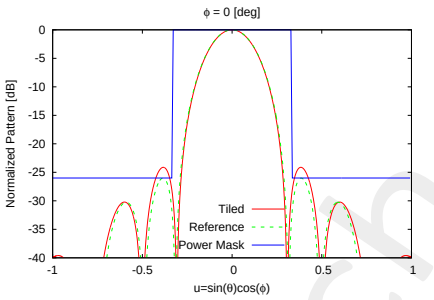	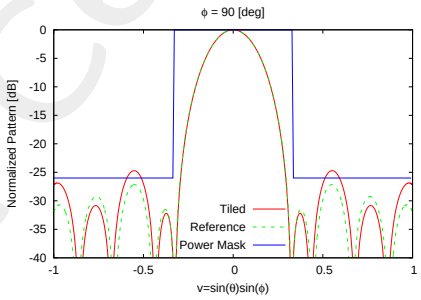
Sol – ID : 99181	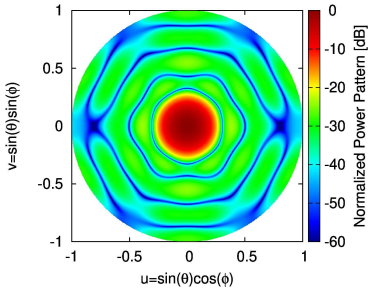	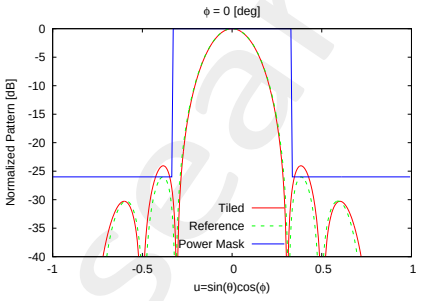	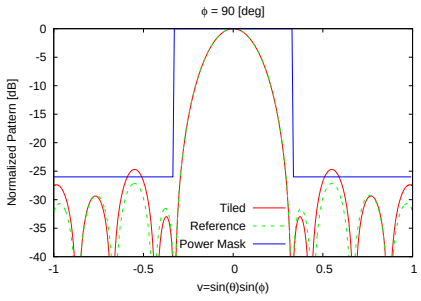
Sol – ID : 99287	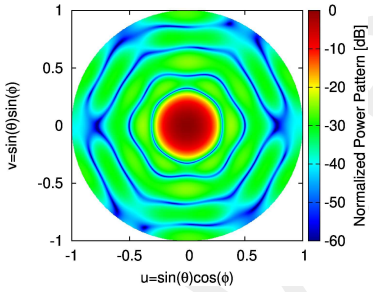	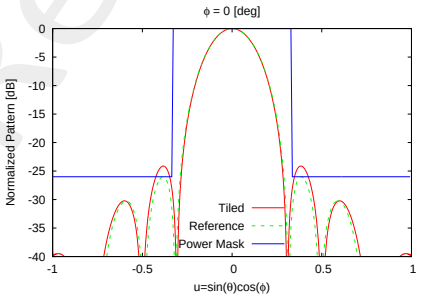	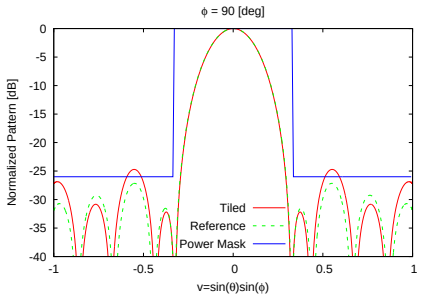

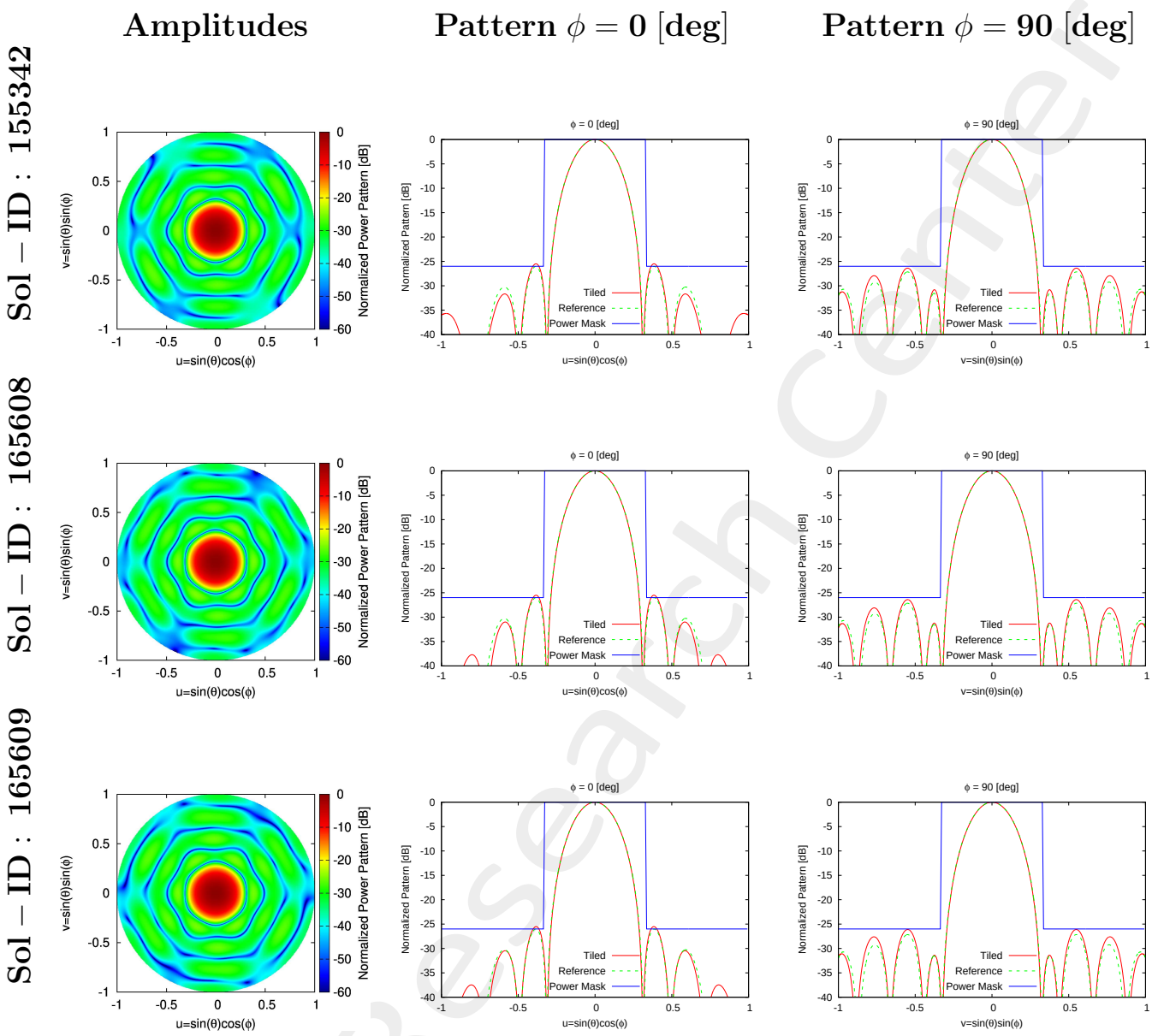

Figure 15: *Mask Matching*, $SLL = -25.99$ $[dB]$, $N_{tot} = 96$, $L_d = 8\lambda$, $d_x = 0.334\lambda$, $d_{y1} = 0.385\lambda$, $d_{y2} = 0.77\lambda$, $a = 4$, $b = 4$, $c = 4$, $(\theta_0, \phi_0) = (0, 0)$ $[deg]$ – Solution ID.: Reference, 95397, 99181, 99287, 155342, 165608, 165609

Steering Analysis

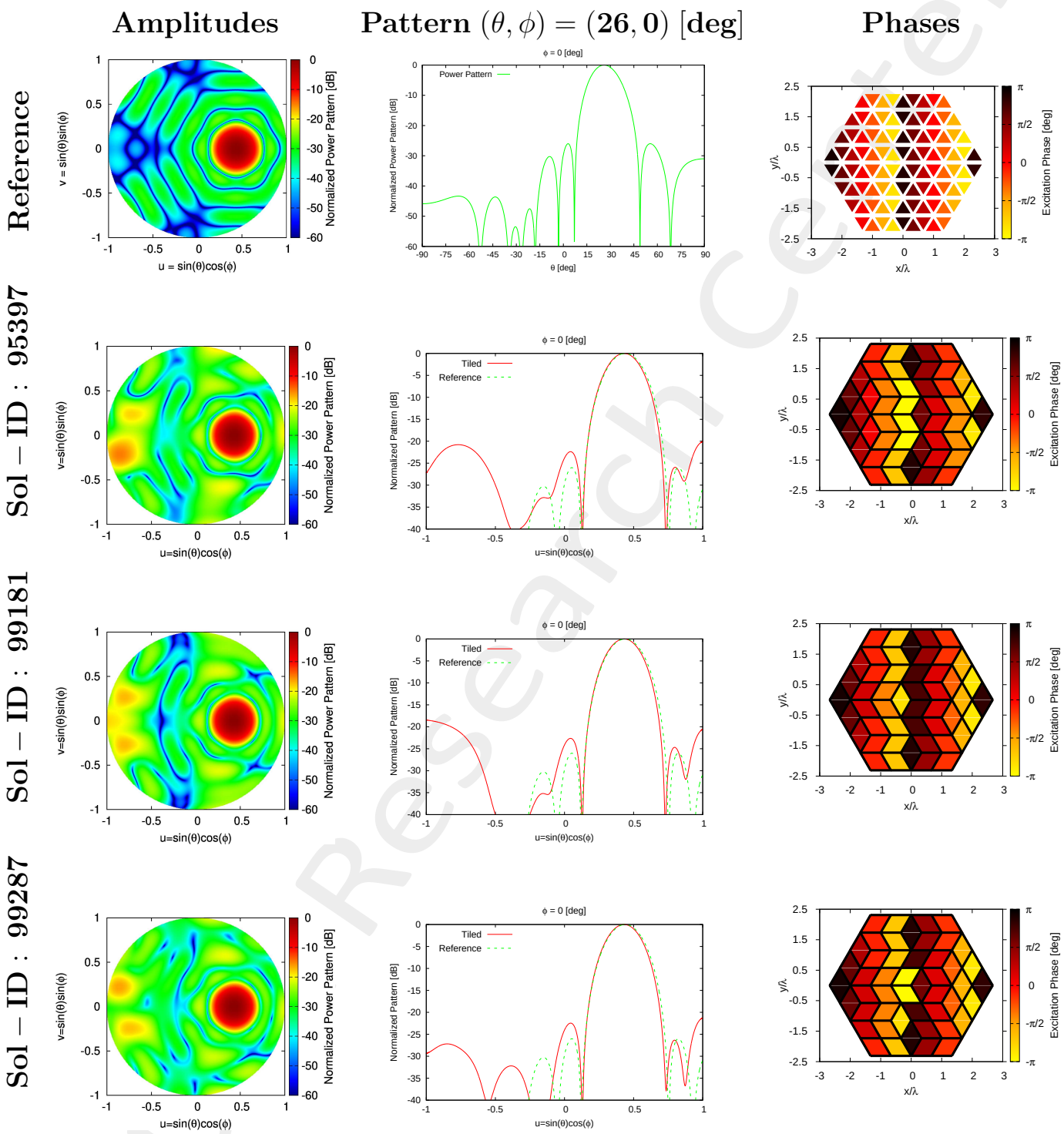

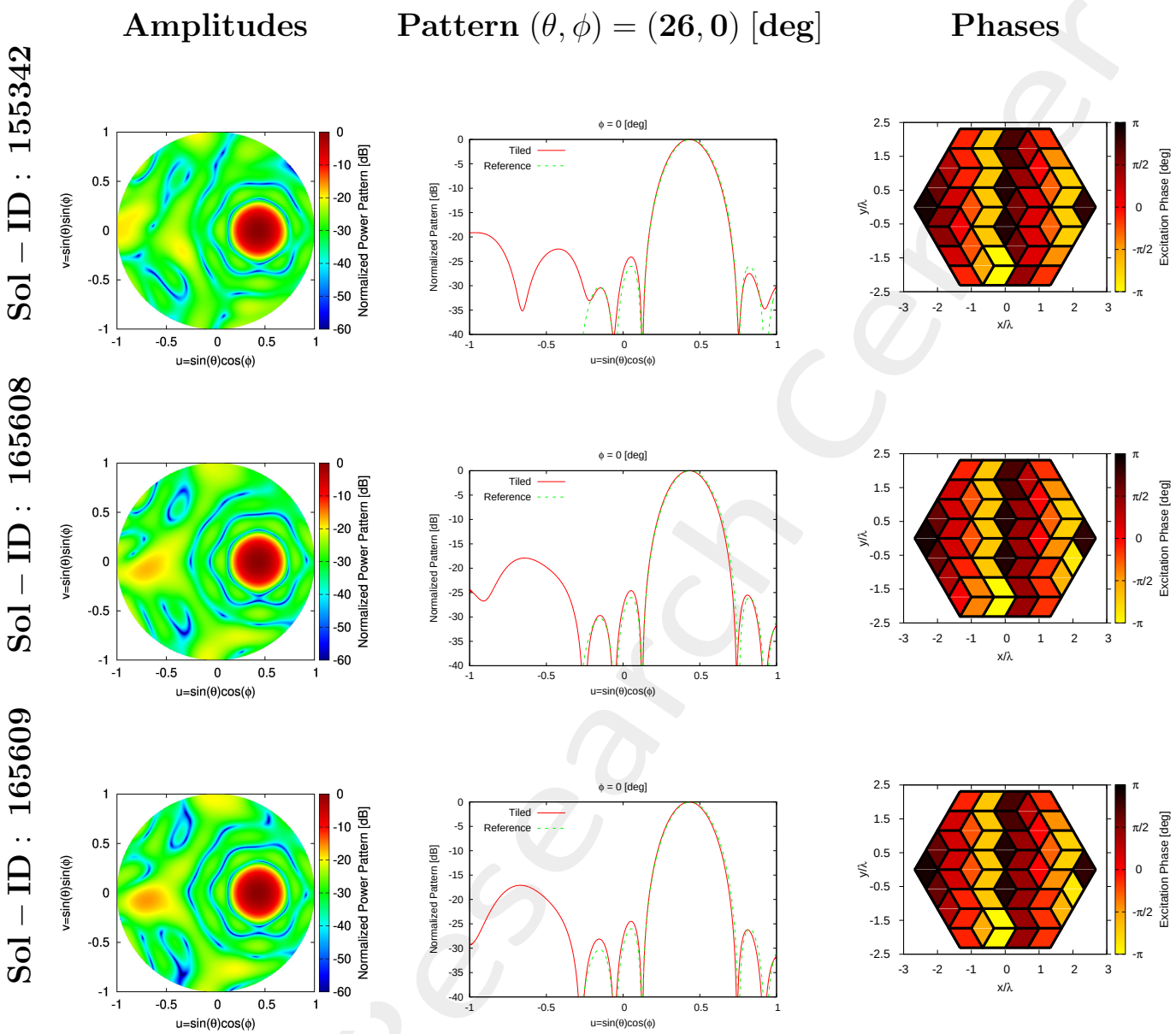

Figure 16: *Mask Matching*, $SLL = -25.99$ $[dB]$, $N_{tot} = 96$, $L_d = 8\lambda$, $d_x = 0.334\lambda$, $d_{y1} = 0.385\lambda$, $d_{y2} = 0.77\lambda$, $a = 4$, $b = 4$, $c = 4$, $(\theta_0, \phi_0) = (26, 0)$ $[deg]$ – Solution ID.: Reference, 95397, 99181, 99287, 155342, 165608, 165609

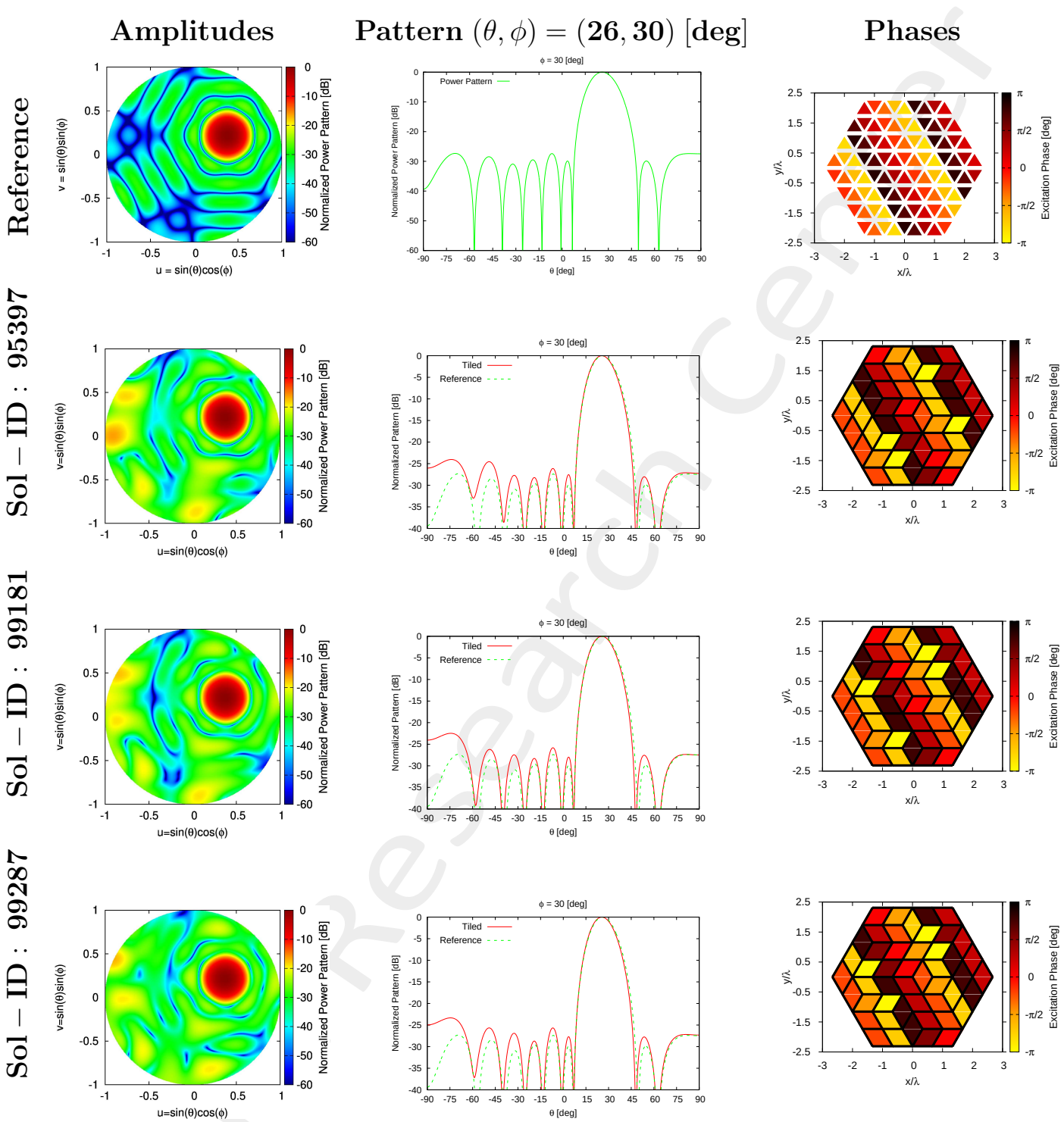

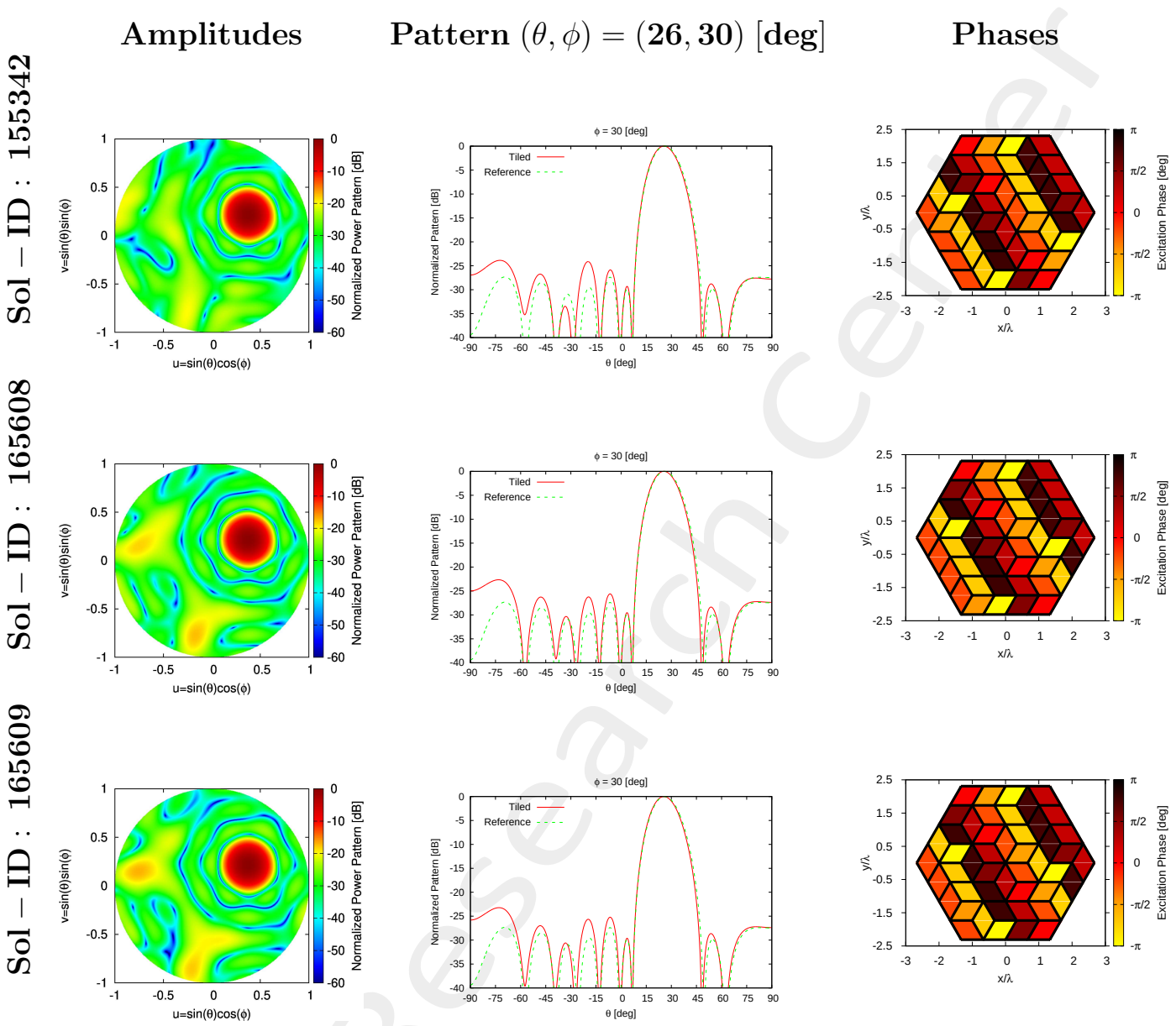

Figure 17: *Mask Matching*, $SLL = -25.99$ $[dB]$, $N_{tot} = 96$, $L_d = 8\lambda$, $d_x = 0.334\lambda$, $d_{y1} = 0.385\lambda$, $d_{y2} = 0.77\lambda$, $a = 4$, $b = 4$, $c = 4$, $(\theta_0, \phi_0) = (26, 30)$ $[deg]$ – Solution ID.: Reference, 95397, 99181, 99287, 155342, 165608, 165609

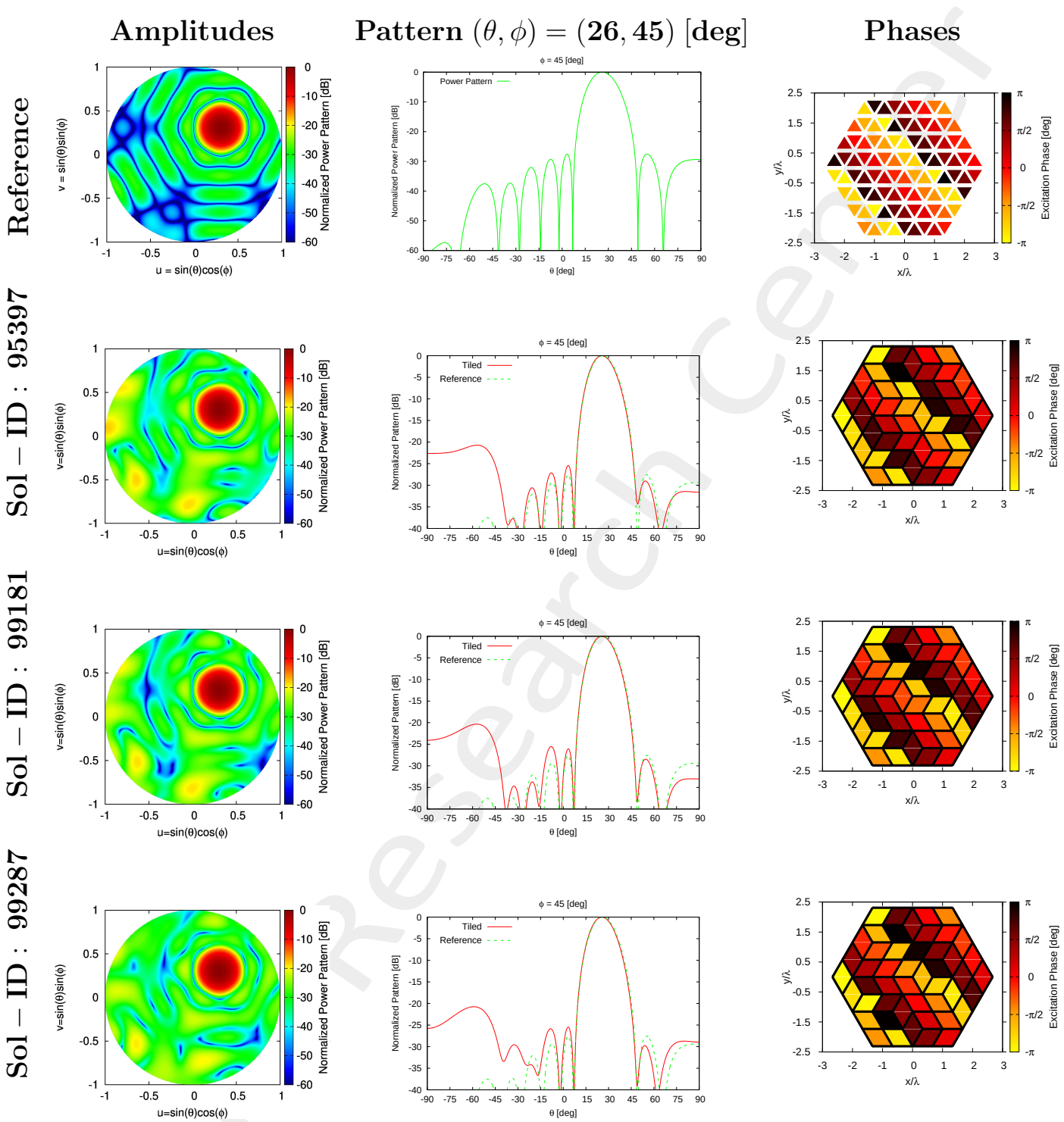

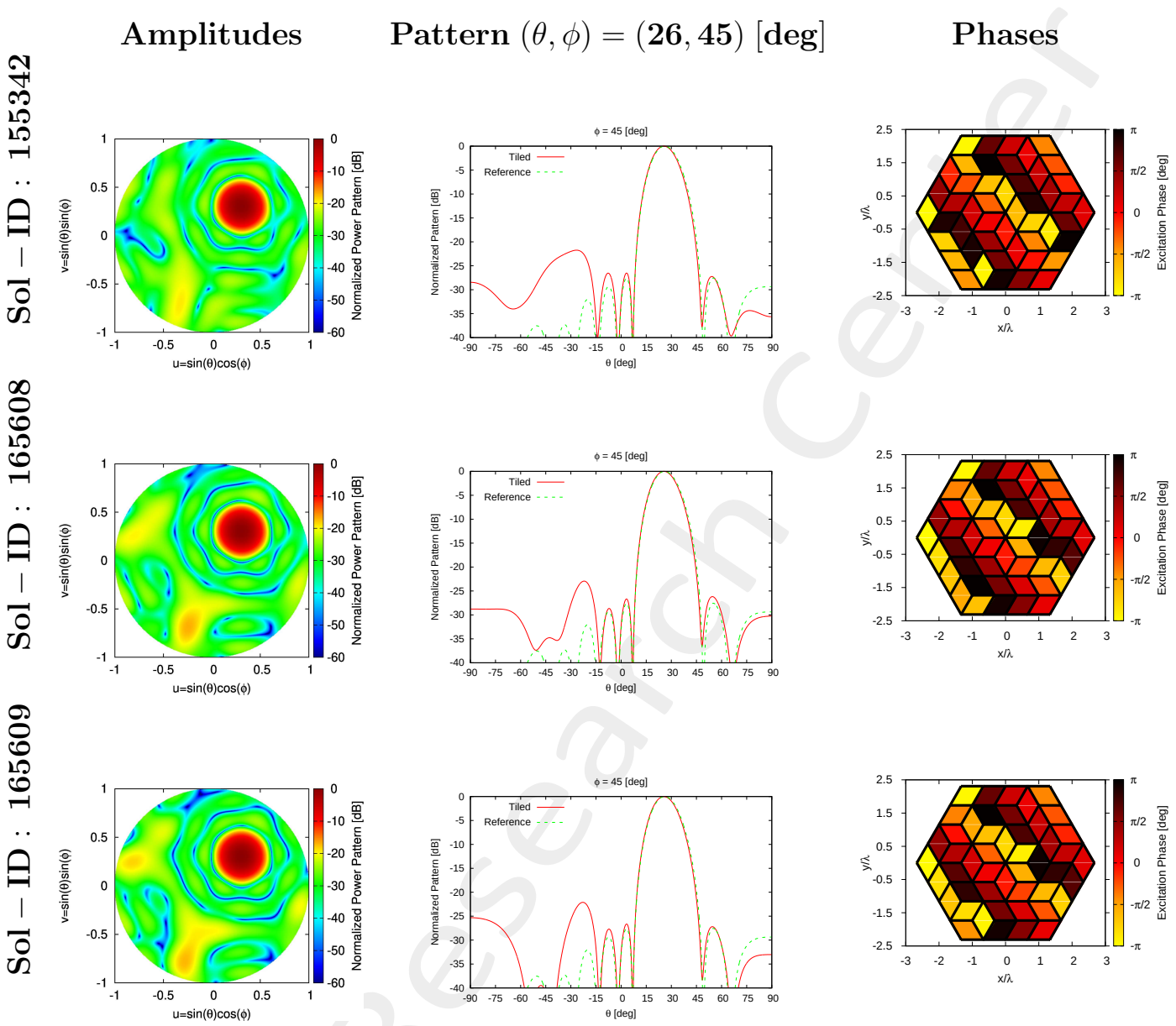

Figure 18: *Mask Matching*, $SLL = -25.99$ $[dB]$, $N_{tot} = 96$, $L_d = 8\lambda$, $d_x = 0.334\lambda$, $d_{y1} = 0.385\lambda$, $d_{y2} = 0.77\lambda$, $a = 4$, $b = 4$, $c = 4$, $(\theta_0, \phi_0) = (26, 45)$ $[deg]$ – Solution ID.: Reference, 95397, 99181, 99287, 155342, 165608, 165609

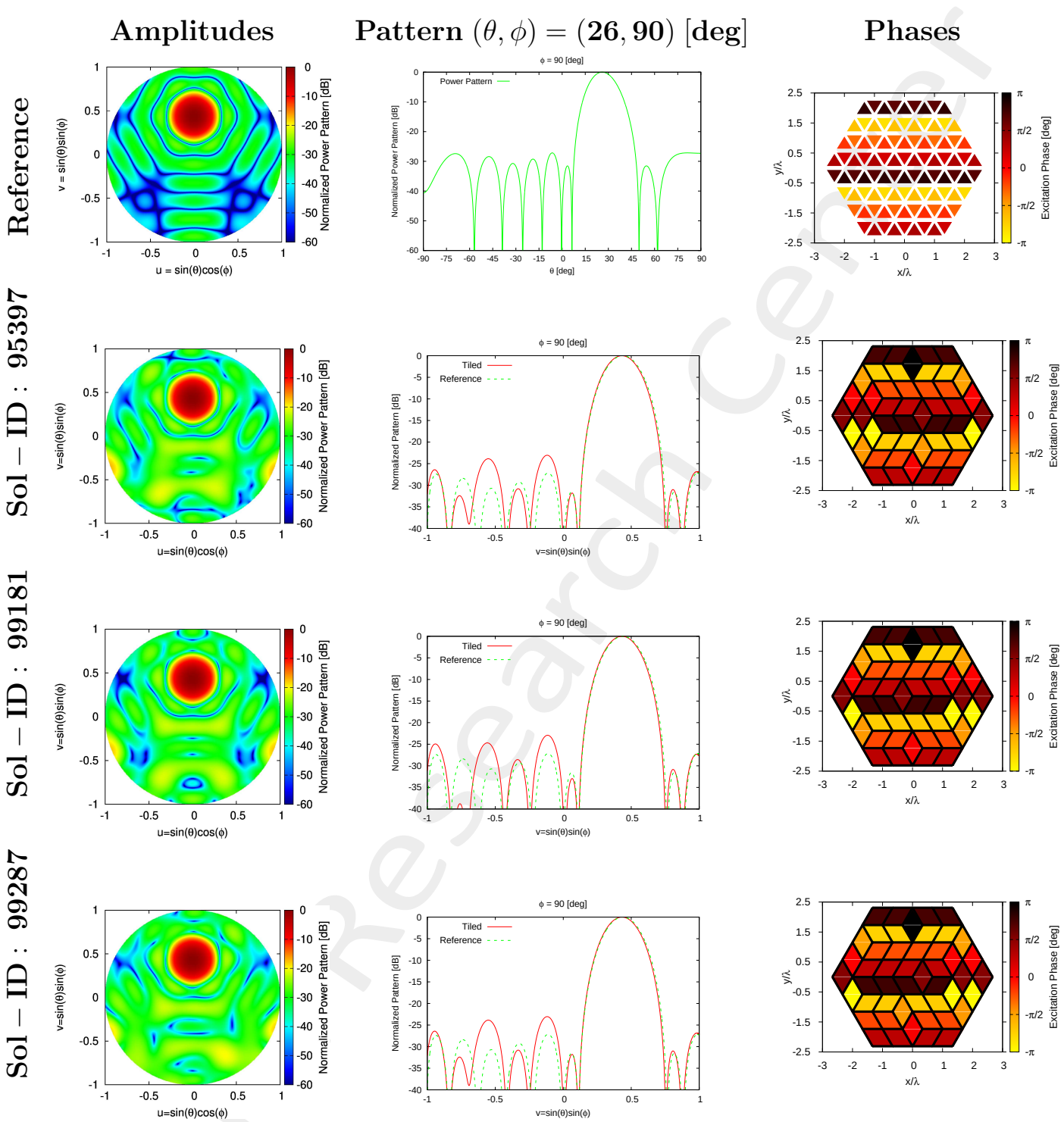

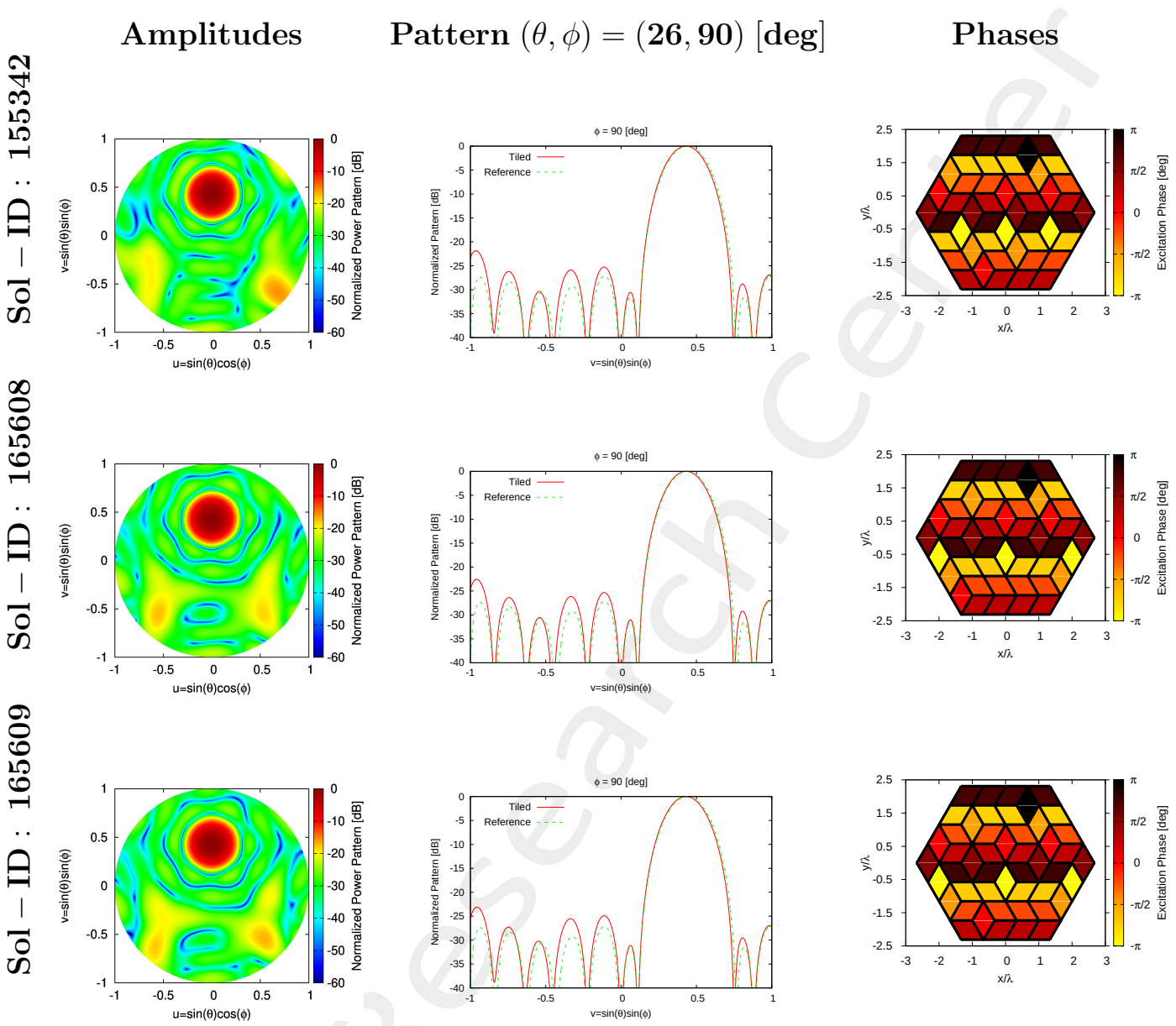

Figure 19: *Mask Matching*, $SLL = -25.99$ $[dB]$, $N_{tot} = 96$, $L_d = 8\lambda$, $d_x = 0.334\lambda$, $d_{y1} = 0.385\lambda$, $d_{y2} = 0.77\lambda$, $a = 4$, $b = 4$, $c = 4$, $(\theta_0, \phi_0) = (26, 90)$ $[deg]$ – Solution ID.: Reference, 95397, 99181, 99287, 155342, 165608, 165609

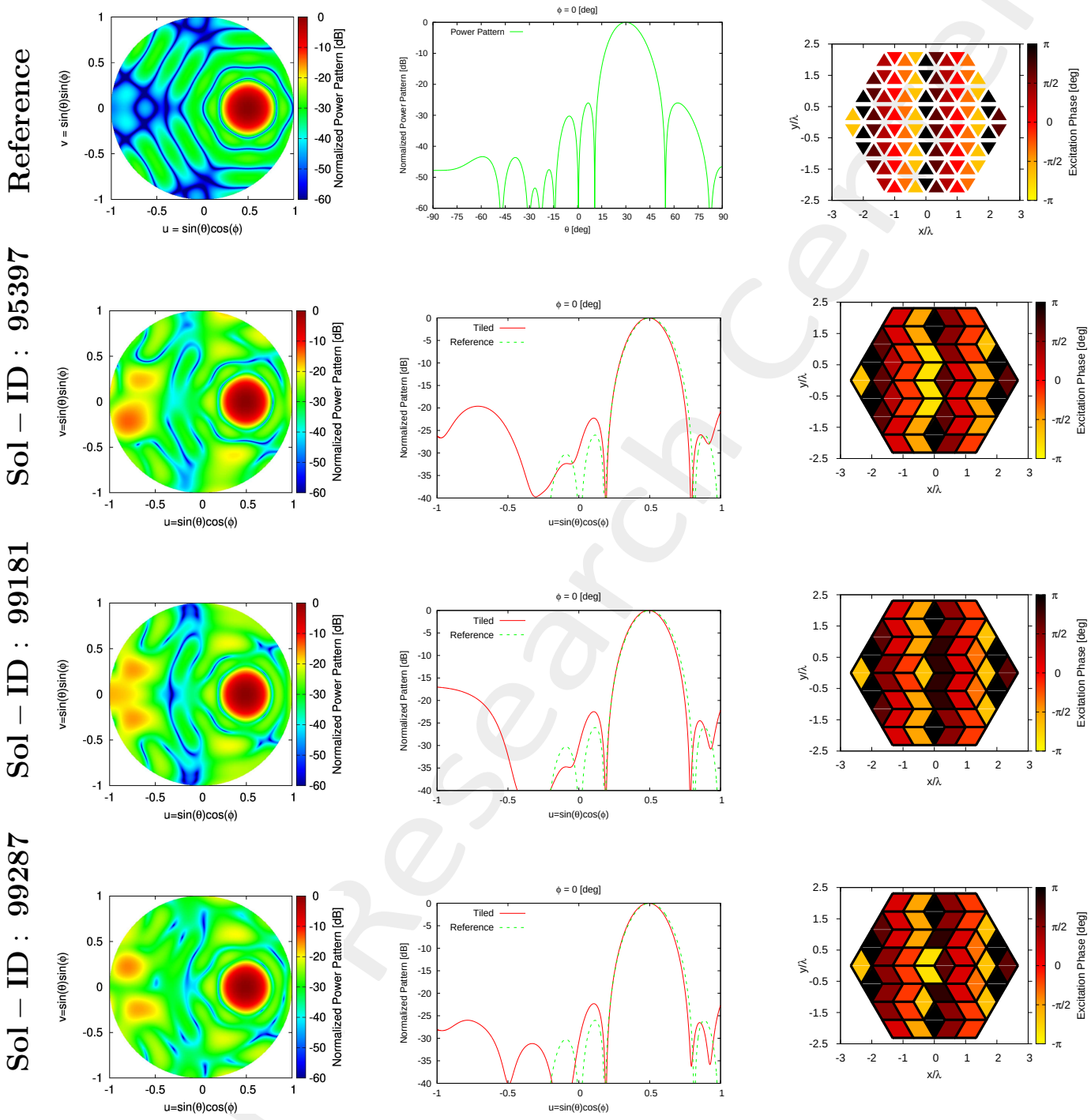

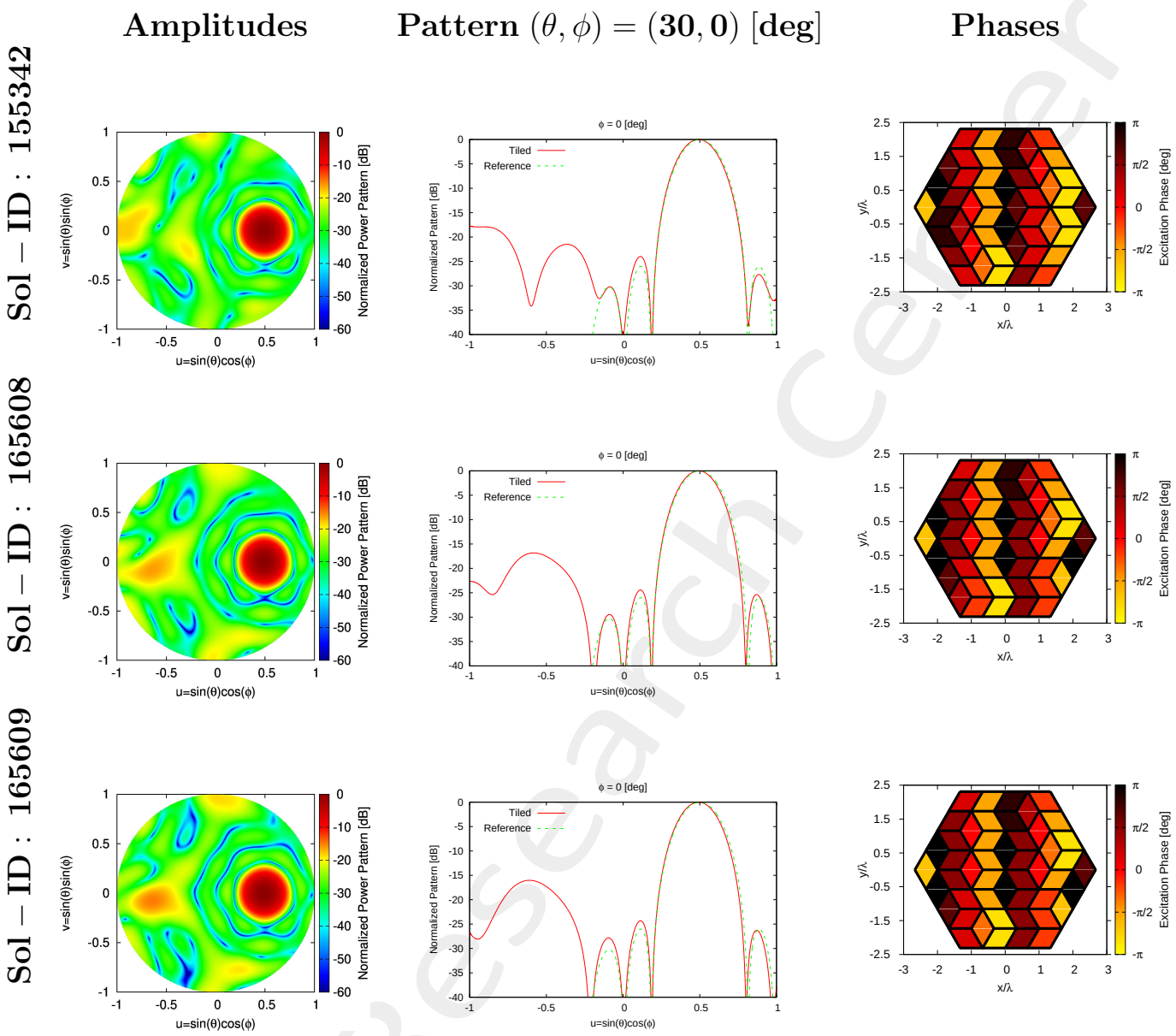

Figure 20: *Mask Matching*, $SLL = -25.99$ $[dB]$, $N_{tot} = 96$, $L_d = 8\lambda$, $d_x = 0.334\lambda$, $d_{y1} = 0.385\lambda$, $d_{y2} = 0.77\lambda$, $a = 4$, $b = 4$, $c = 4$, $(\theta_0, \phi_0) = (30, 0)$ $[deg]$ – Solution ID.: Reference, 95397, 99181, 99287, 155342, 165608, 165609

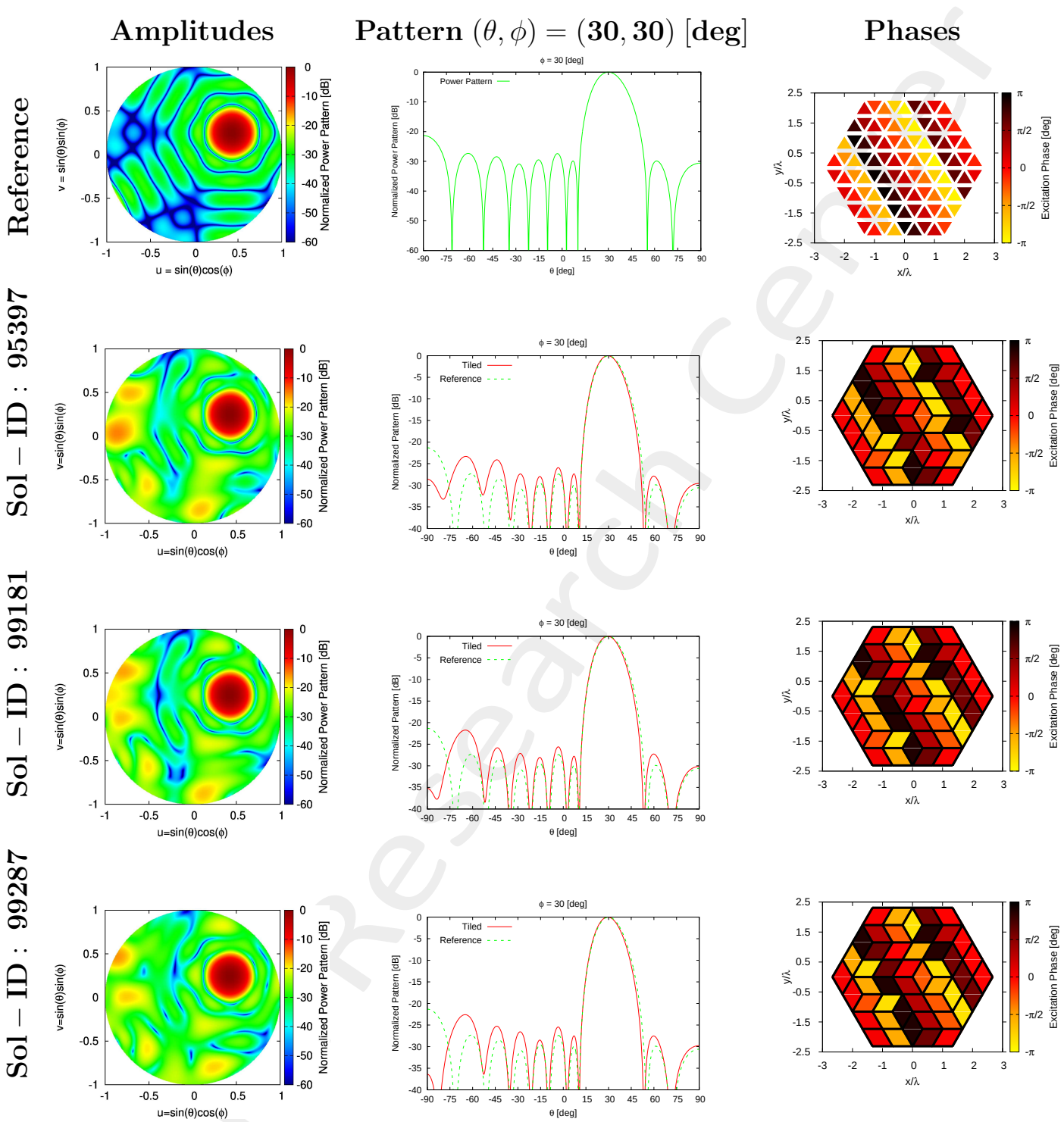

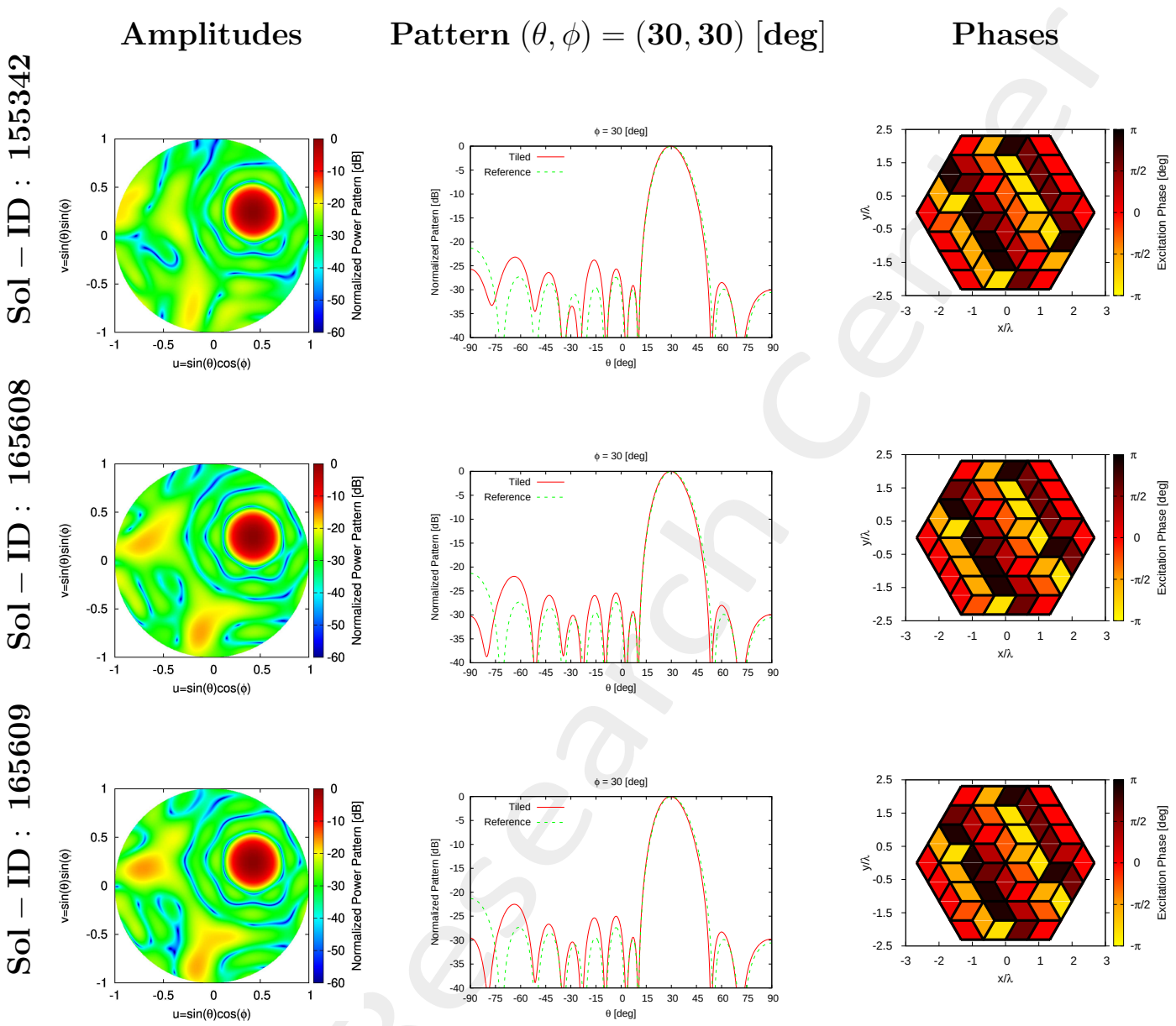

Figure 21: *Mask Matching*, $SLL = -25.99$ $[dB]$, $N_{tot} = 96$, $L_d = 8\lambda$, $d_x = 0.334\lambda$, $d_{y1} = 0.385\lambda$, $d_{y2} = 0.77\lambda$, $a = 4$, $b = 4$, $c = 4$, $(\theta_0, \phi_0) = (30, 30)$ $[deg]$ − Solution ID.: Reference, 95397, 99181, 99287, 155342, 165608, 165609

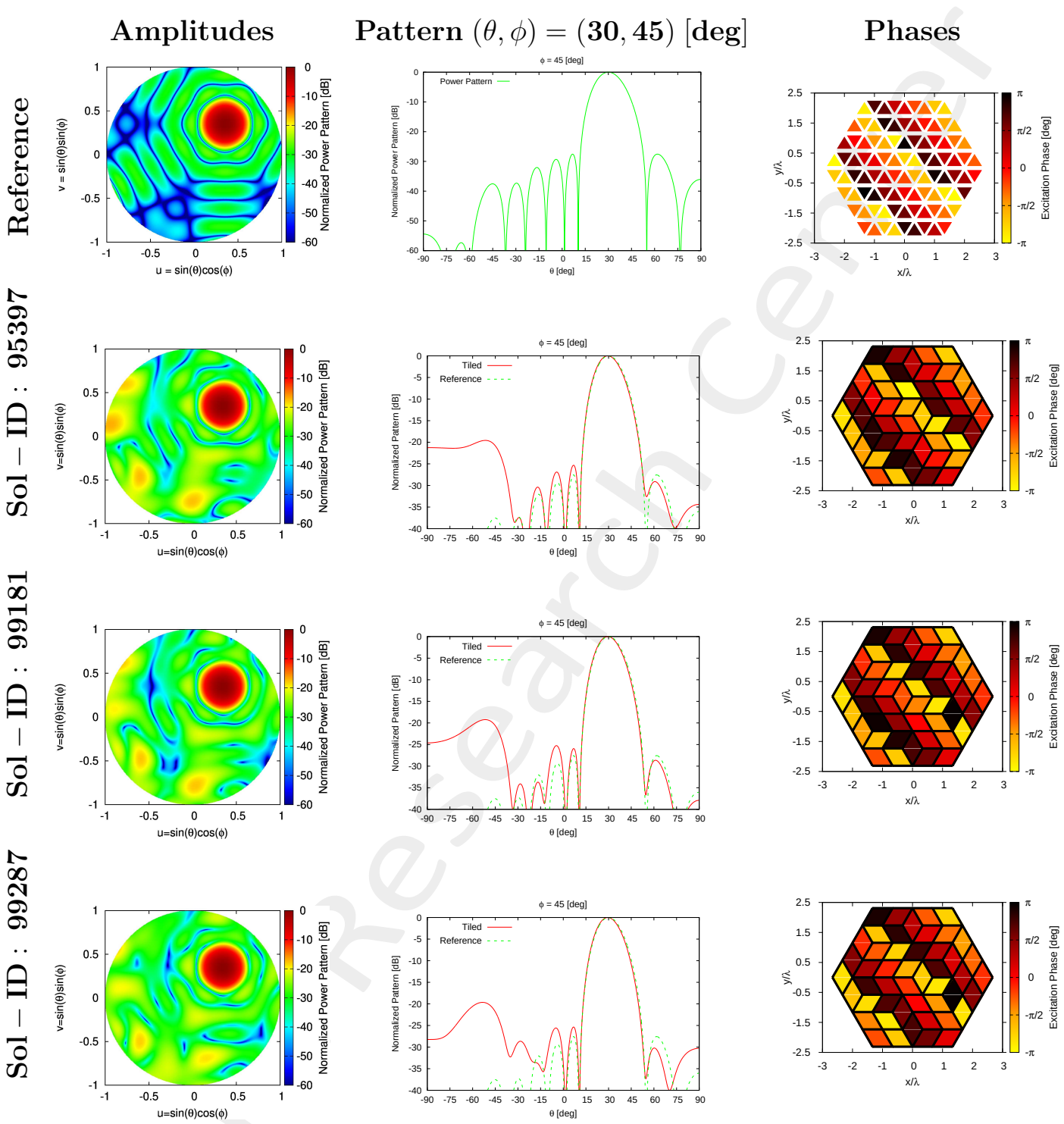

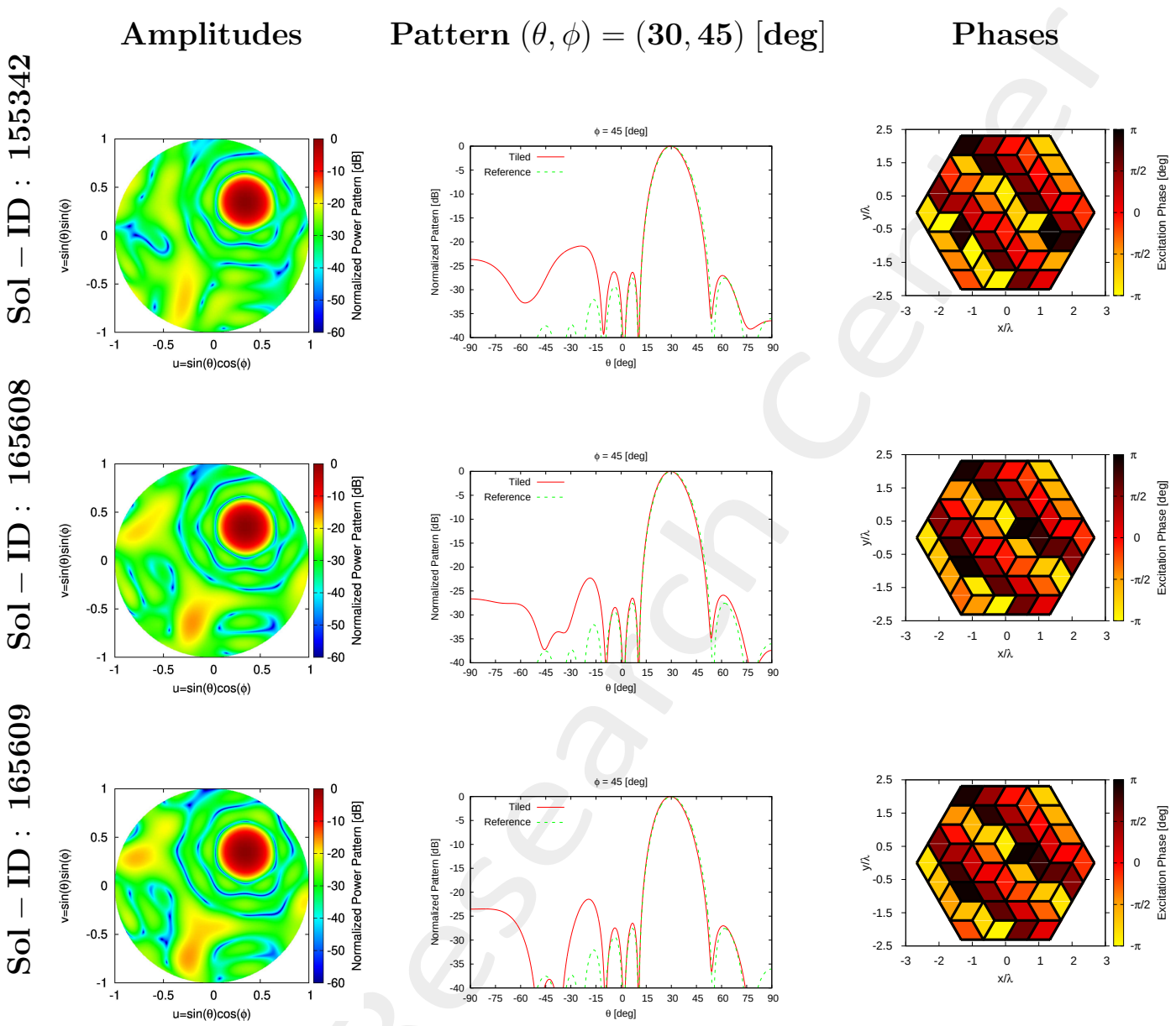

Figure 22: *Mask Matching*, $SLL = -25.99$ $[dB]$, $N_{tot} = 96$, $L_d = 8\lambda$, $d_x = 0.334\lambda$, $d_{y1} = 0.385\lambda$, $d_{y2} = 0.77\lambda$, $a = 4$, $b = 4$, $c = 4$, $(\theta_0, \phi_0) = (30, 45)$ $[deg]$ – Solution ID.: Reference, 95397, 99181, 99287, 155342, 165608, 165609

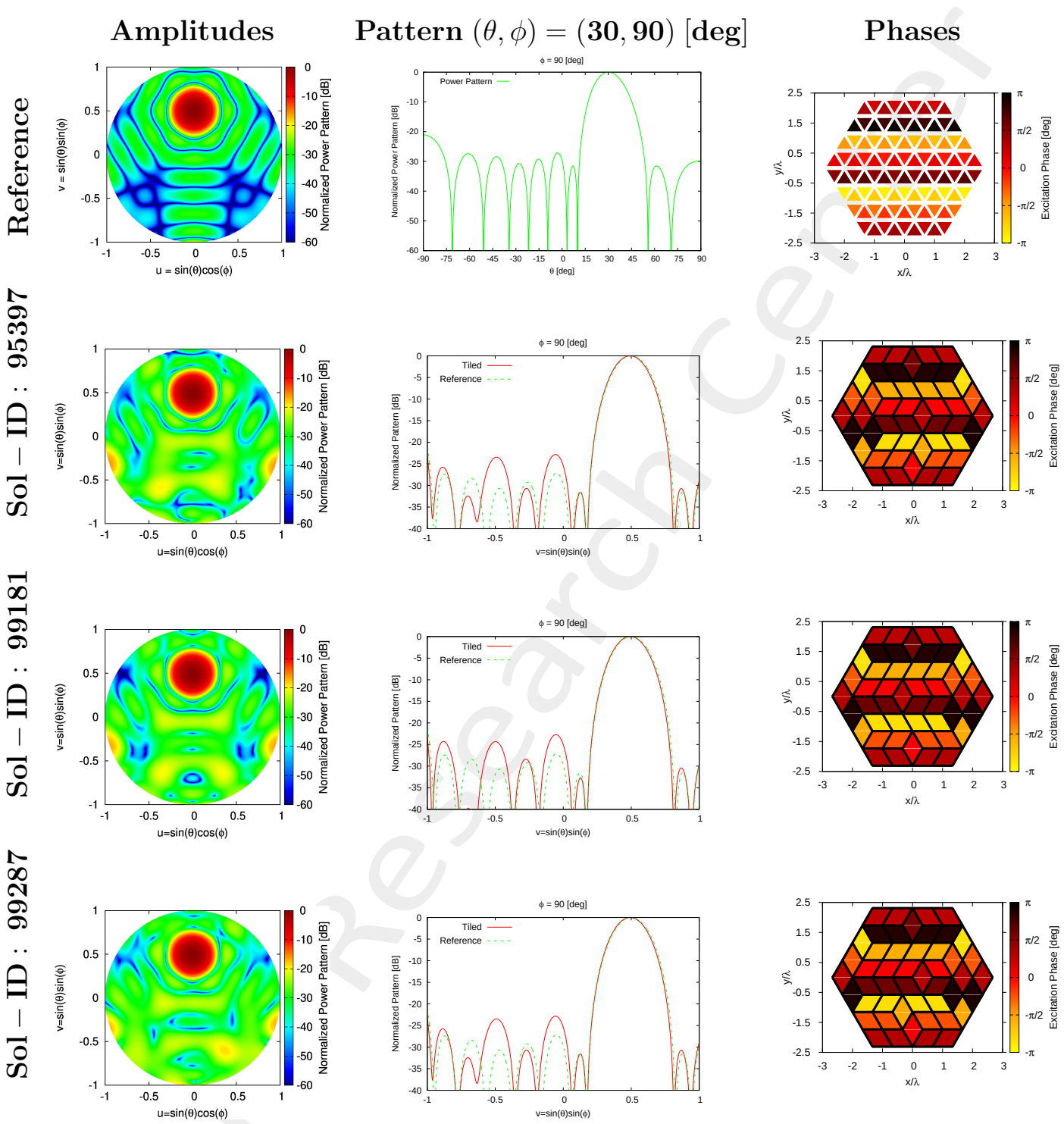

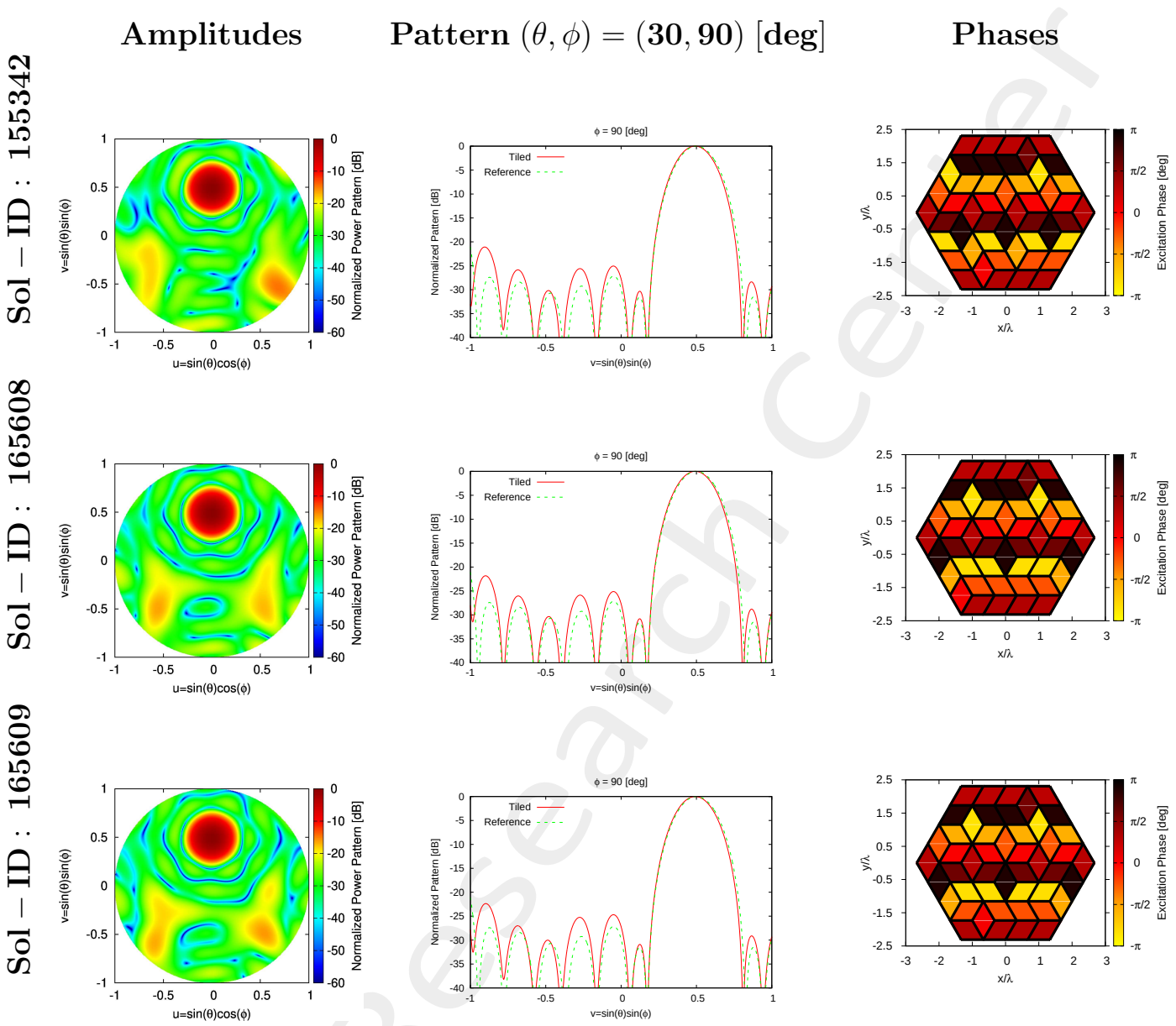

Figure 23: *Mask Matching*, $SLL = -25.99$ $[dB]$, $N_{tot} = 96$, $L_d = 8\lambda$, $d_x = 0.334\lambda$, $d_{y1} = 0.385\lambda$, $d_{y2} = 0.77\lambda$, $a = 4$, $b = 4$, $c = 4$, $(\theta_0, \phi_0) = (30, 90)$ $[deg]$ – Solution ID.: Reference, 95397, 99181, 99287, 155342, 165608, 165609

Solutions Summary

(a, b, c)	**T** (# tilings)	$\triangle\tau$ $[sec]$ (single simulation period)	τ $[sec]$ total simulation period
4, 4, 4	232848	0.072159	16802.173

Table 32: Simulation Time

SOLUTION ID	**SLL** [dB]	**HPBW** (azimuth) [deg]	**HPBW** (elevation) [deg]	**D** [dB]	**Mask Fitting**
Reference	−25.985	13.922	13.970	22.942	0
95397	−24.121	13.816	13.903	22.937	2.599×10^{-5}
99181	−24.052	13.821	13.914	22.934	2.599×10^{-5}
99287	−24.120	13.816	13.903	22.937	2.599×10^{-5}
155342	−25.116	13.857	13.905	22.939	1.999×10^{-6}
165608	−25.199	13.859	13.920	22.953	1.999×10^{-6}
165609	−25.443	13.853	13.911	22.945	1.999×10^{-6}

Table 33: SLL, $HPBW_{az}$, $HPBW_{el}$, D, *Mask Fitting of Radiation Pattern* along $(\theta_0, \phi_0) = (0, 0)$ $[deg]$

More information on the topics of this document can be found in the following list of references.

References

[1] P. Rocca, M. Benedetti, M. Donelli, D. Franceschini, and A. Massa, "Evolutionary optimization as applied to inverse problems," *Inverse Problems - 25 th Year Special Issue of Inverse Problems, Invited Topical Review*, vol. 25, pp. 1-41, Dec. 2009

[2] P. Rocca, G. Oliveri, and A. Massa, "Differential Evolution as applied to electromagnetics," *IEEE Antennas Propag. Mag.*, vol. 53, no. 1, pp. 38-49, Feb. 2011

[3] P. Rocca, N. Anselmi, A. Polo, and A. Massa, "An irregular two-sizes square tiling method for the design of isophoric phased arrays," *IEEE Trans. Antennas Propag.*, vol. 68, no. 6, pp. 4437-4449, Jun. 2020

[4] P. Rocca, N. Anselmi, A. Polo, and A. Massa, "Modular design of hexagonal phased arrays through diamond tiles," *IEEE Trans. Antennas Propag.*, vol.68, no. 5, pp. 3598-3612, May 2020

[5] N. Anselmi, L. Poli, P. Rocca, and A. Massa, "Design of simplified array layouts for preliminary experimental testing and validation of large AESAs," *IEEE Trans. Antennas Propag.*, vol. 66, no. 12, pp. 6906-6920, Dec. 2018

[6] N. Anselmi, P. Rocca, M. Salucci, and A. Massa, "Contiguous phase-clustering in multibeam-on-receive scanning arrays," *IEEE Trans. Antennas Propag.*, vol. 66, no. 11, pp. 5879-5891, Nov. 2018

[7] G. Oliveri, G. Gottardi, F. Robol, A. Polo, L. Poli, M. Salucci, M. Chuan, C. Massagrande, P. Vinetti, M. Mattivi, R. Lombardi, and A. Massa, "Co-design of unconventional array architectures and antenna elements for 5G base station," *IEEE Trans. Antennas Propag.*, vol. 65, no. 12, pp. 6752-6767, Dec. 2017

[8] N. Anselmi, P. Rocca, M. Salucci, and A. Massa, "Irregular phased array tiling by means of analytic schemata-driven optimization," *IEEE Trans. Antennas Propag.*, vol. 65, no. 9, pp. 4495-4510, September 2017

[9] N. Anselmi, P. Rocca, M. Salucci, and A. Massa, "Optimization of excitation tolerances for robust beamforming in linear arrays," *IET Microwaves, Antennas & Propagation*, vol. 10, no. 2, pp. 208-214, 2016

[10] P. Rocca, R. J. Mailloux, and G. Toso, "GA-Based optimization of irregular sub-array layouts for wideband phased arrays desig," *IEEE Antennas and Wireless Propag. Lett.*, vol. 14, pp. 131-134, 2015

[11] P. Rocca, M. Donelli, G. Oliveri, F. Viani, and A. Massa, "Reconfigurable sum-difference pattern by means of parasitic elements for forward-looking monopulse radar," *IET Radar, Sonar & Navigation*, vol 7, no. 7, pp. 747-754, 2013

[12] P. Rocca, L. Manica, and A. Massa, "Ant colony based hybrid approach for optimal compromise sum-difference patterns synthesis," *Microwave Opt. Technol. Lett.*, vol. 52, no. 1, pp. 128-132, Jan. 2010

[13] P. Rocca, L. Manica, and A. Massa, "An improved excitation matching method based on an ant colony optimization for suboptimal-free clustering in sum-difference compromise synthesis," *IEEE Trans. Antennas Propag.*, vol. 57, no. 8, pp. 2297-2306, Aug. 2009

[14] M. Salucci, L. Poli, A. F. Morabito, and P. Rocca, "Adaptive nulling through subarray switching in planar antenna arrays," *Journal of Electromagnetic Waves and Applications*, vol. 30, no. 3, pp. 404-414, February 2016

[15] T. Moriyama, L. Poli, and P. Rocca, "Adaptive nulling in thinned planar arrays through genetic algorithms," *IEICE Electronics Express*, vol. 11, no. 21, pp. 1-9, Sep. 2014

[16] L. Poli, P. Rocca, M. Salucci, and A. Massa, "Reconfigurable thinning for the adaptive control of linear arrays," *IEEE Trans. Antennas Propag.*, vol. 61, no. 10, pp. 5068-5077, Oct. 2013

[17] P. Rocca, L. Poli, G. Oliveri, and A. Massa, "Adaptive nulling in time-varying scenarios through time-modulated linear arrays," *IEEE Antennas Wireless Propag. Lett.*, vol. 11, pp. 101-104, 2012

[18] M. Benedetti, G. Oliveri, P. Rocca, and A. Massa, "A fully-adaptive smart antenna prototype: ideal model and experimental validation in complex interference scenarios," *Progress in Electromagnetic Research*, PIER 96, pp. 173-191, 2009

[19] P. Rocca, L. Poli, A. Polo, and A. Massa, "Optimal excitation matching strategy for sub-arrayed phased linear arrays generating arbitrary shaped beams," *IEEE Trans. Antennas Propag.*, vol. 68, no. 6, pp. 4638-4647, Jun. 2020

[20] G. Oliveri, G. Gottardi and A. Massa, "A new meta-paradigm for the synthesis of antenna arrays for future wireless communications," *IEEE Trans. Antennas Propag.*, vol. 67, no. 6, pp. 3774-3788, Jun. 2019

[21] P. Rocca, M. H. Hannan, L. Poli, N. Anselmi, and A. Massa, "Optimal phase-matching strategy for beam scanning of sub-arrayed phased arrays," *IEEE Trans. Antennas and Propag.*, vol. 67, no. 2, pp. 951-959, Feb. 2019

[22] L. Poli, G. Oliveri, P. Rocca, M. Salucci, and A. Massa, "Long-Distance WPT Unconventional Arrays Synthesis," *Journal of Electromagnetic Waves and Applications*, vol. 31, no. 14, pp. 1399-1420, Jul. 2017

[23] G. Gottardi, L. Poli, P. Rocca, A. Montanari, A. Aprile, and A. Massa, "Optimal Monopulse Beamforming for Side-Looking Airborne Radars," *IEEE Antennas Wireless Propag. Lett.*, vol. 16, pp. 1221-1224, 2017

[24] G. Oliveri, M. Salucci, and A. Massa, "Synthesis of modular contiguously clustered linear arrays through a sparseness-regularized solver," *IEEE Trans. Antennas Propag.*, vol. 64, no. 10, pp. 4277-4287, Oct. 2016

[25] P. Rocca, G. Oliveri, R. J. Mailloux, and A. Massa, "Unconventional phased array architectures and design Methodologies - A review," *Proceedings of the IEEE = Special Issue on 'Phased Array Technologies', Invited Paper*, vol. 104, no. 3, pp. 544-560, March 2016

[26] P. Rocca, M. D'Urso, and L. Poli, "Advanced strategy for large antenna array design with subarray-only amplitude and phase contr," *IEEE Antennas and Wireless Propag. Lett.*, vol. 13, pp. 91-94, 2014

[27] L. Manica, P. Rocca, G. Oliveri, and A. Massa, "Synthesis of multi-beam sub-arrayed antennas through an excitation matching strategy," *IEEE Trans. Antennas Propag.*, vol. 59, no. 2, pp. 482-492, Feb. 2011

[28] G. Oliveri, "Multi-beam antenna arrays with common sub-array layouts," *IEEE Antennas Wireless Propag. Lett.*, vol. 9, pp. 1190-1193, 2010

[29] P. Rocca, R. Haupt, and A. Massa, "Sidelobe reduction through element phase control in sub-arrayed array antennas," *IEEE Antennas Wireless Propag. Lett.*, vol. 8, pp. 437-440, 2009

[30] P. Rocca, L. Manica, R. Azaro, and A. Massa, "A hybrid approach for the synthesis of sub-arrayed monopulse linear arrays," *IEEE Trans. Antennas Propag.*, vol. 57, no. 1, pp. 280-283, Jan. 2009

[31] L. Manica, P. Rocca, M. Benedetti, and A. Massa, "A fast graph-searching algorithm enabling the efficient synthesis of sub-arrayed planar monopulse antennas," *IEEE Trans. Antennas Propag.*, vol. 57, no. 3, pp. 652-664, Mar. 2009

[32] P. Rocca, L. Manica, A. Martini, and A. Massa, "Compromise sum-difference optimization through the iterative contiguous partition method," *IET Microwaves, Antennas & Propagation*, vol. 3, no. 2, pp. 348-361, 2009

[33] L. Manica, P. Rocca, and A. Massa, "An excitation matching procedure for sub-arrayed monopulse arrays with maximum directivity," *IET Radar, Sonar & Navigation*, vol. 3, no. 1, pp. 42-48, Feb. 2009

[34] L. Manica, P. Rocca, and A. Massa, "Design of subarrayed linear and planar array antennas with SLL control based on an excitation matching approach," *IEEE Trans. Antennas Propag.*, vol. 57, no. 6, pp. 1684-1691, Jun. 2009